COMPARISON OF ^{14}C AND U-Th AGES IN CORALS FROM IODP #310 CORES OFFSHORE TAHITI

Nicolas Durand[1,2] • Pierre Deschamps[1] • Edouard Bard[1] • Bruno Hamelin[1] • Gilbert Camoin[1] • Alexander L Thomas[3] • Gideon M Henderson[3] • Yusuke Yokoyama[4,5] • Hiroyuki Matsuzaki[6]

ABSTRACT. Shallow-water tropical corals can be used to calibrate the radiocarbon timescale. In this paper, we present a new data set based on the comparison between ^{14}C ages and U-Th ages measured in fossil corals collected offshore the island of Tahiti during the Integrated Oceanic Drilling Program (IODP) Expedition 310. After applying strict mineralogical and geochemical screening criteria, the Tahiti record provides new data for 2 distinct time windows: 7 data for the interval between 29 and 37 cal kyr BP and 58 for the last deglaciation period, notably a higher resolution for the 14–16 cal kyr BP time interval. There are 3 main outcomes of this study. First, it extends the previous Tahiti record beyond 13.9 cal kyr BP, the oldest U-Th age obtained on cores drilled onshore in the modern Tahiti barrier reef. Second, it strengthens the data set of the 14–15 cal kyr BP period, allowing for better documentation of the ^{14}C age plateau in this time range. This age plateau corresponds to a drop of the atmospheric ^{14}C synchronous with an abrupt period of sea-level rise (Melt Water Pulse 1A, MWP-1A). The Tahiti ^{14}C record documents complex changes in the global carbon cycle due to variations in the exchange rates between its different reservoirs. Third, during the Heinrich event 1, the Tahiti record disagrees with the Cariaco record, but is in broad agreement with other marine and continental data.

INTRODUCTION

For the period covering the last 50,000 yr, the radiocarbon clock is the most widely used dating tool in disciplines such as archaeology and paleoclimatology. However, the reliability of the ^{14}C time-scale depends on precise knowledge of past changes in the atmospheric ^{14}C/^{12}C ratio. This ratio is controlled by variations in the ^{14}C production rate due to changes in the Earth's magnetic field and/or variability of solar activity, as well as rearrangements between the different reactive reservoirs of the carbon cycle. Accurately and independently dated records of past atmospheric ^{14}C concentration (usually expressed as Δ^{14}C, the decay-corrected deviation, in ‰, from the standard pre-industrial atmospheric ^{14}C concentration, see Stuiver and Polach 1977) are thus essential to correct for these ^{14}C fluctuations through time and therefore calibrate the ^{14}C timescale. In turn, this calibration curve provides crucial information to compute past variations in atmospheric ^{14}C production rate, and to constrain the exchanges of carbon between surface reservoirs (atmosphere, biosphere, and ocean) or to reconstruct past fluctuation of oceanic circulation and ventilation.

For the Holocene period, the ^{14}C timescale is reliably calibrated through the use of dendro-dated tree rings. This approach provides continuous records of past atmospheric ^{14}C from present day to 12,594 cal kyr BP (Friedrich et al. 2004b; Schaub et al. 2008b). Additional floating tree-ring sequences extend the tree-ring record back to about 14 cal kyr BP (Friedrich et al. 2004a; Schaub et al. 2008a,b; Hua et al. 2009). Older floating series are available, but they remain too scarce, and their distribution too patchy, to produce a continuous record (Hogg et al. 2006; Palmer et al. 2006; Stambaugh and Guyette 2009). Beyond the range of the tree-ring record, and with the exception of terrestrial macrofossils (leaves, branches, and insects) recovered in varved lacustrine sediments (Gos-

[1]CEREGE, Aix-Marseille Univ., CNRS, IRD, Collège de France, Technopole de l'Arbois, BP 80, 13545 Aix-en-Provence Cedex 4, France.
[2]Present address: Laboratoire de Mesure du Carbone 14 UMS 2572, CEA-Saclay, Bât. 450, 91191 Gif-sur-Yvette Cedex, France. Corresponding author: nicolas.durand@cea.fr.
[3]Department of Earth Sciences, South Parks Road, Oxford OX1 3AN, United Kingdom.
[4]Atmosphere and Ocean Research Institute and Department of Earth and Planetary Science University of Tokyo, 5-1-5 Kashiwanoha, Kashiwashi, Chiba 277-8564, Japan.
[5]Institute of Biogeosciences, JAMSTEC, Yokosuka, Japan.
[6]Department of Nuclear Engineering and Management, University of Tokyo, 2-11-16 Yayoi, Tokyo 113-0032, Japan.

lar et al. 1995; Kitagawa and van der Plicht 2000), ^{14}C calibration is mainly derived from continental or marine carbonate archives: speleothems (e.g. Hoffmann et al. 2010; Southon et al. 2012); corals (e.g. Bard et al. 1990a,b; Edwards et al. 1993); and foraminifera (e.g. Hughen et al. 1998, 2006; Bard et al. 2004a,b; Shackleton et al. 2004). However, these records do not provide a direct measurement of atmospheric ^{14}C content. Speleothem records, for example, must be corrected for a significant contribution of dead (or geologic) carbon, with the questionable assumption that this dead carbon fraction did not significantly vary over the glacial cycle (Hoffmann et al. 2010; Southon et al. 2012). For marine archives, the raw data need to be corrected for the marine reservoir age effect that accounts for the difference between the atmosphere and local seawater ^{14}C, which is due to the balance between the rate of air-sea gas exchanges and the mixing of ^{14}C-depleted subsurface waters. Moreover, this effect may have varied in the past and can be site-specific (Bard 1988). Still, marine archives present the advantage of covering the complete ^{14}C time window. In this respect, fossil corals have been regarded as one of the best candidates for extending the ^{14}C calibration because they are the most suitable material for combining high-accuracy and -precision U-Th dating and ^{14}C age measurements (Bard et al. 1990a,b, 1993, 1998; Edwards et al. 1993; Cutler et al. 2004; Paterne et al. 2004; Fairbanks et al. 2005). This approach, however, is limited by the scarcity of adequate coral sequences that cover the ^{14}C timescale beyond the tree-ring records: corals that thrived during the last glaciation or during marine isotope stage 3 are now as much as 100 m below present sea level.

In this paper, we present a new data set based on paired ^{14}C and absolute U-Th dating of fossil shallow-water tropical corals collected during the Integrated Oceanic Drilling Program (IODP) Expedition 310 "Tahiti Sea-Level" (Camoin et al. 2007a,b). This international offshore drilling campaign, conducted on the Tahiti reef slope, recovered well-preserved high-resolution coral sequences that cover key intervals of the last glacial cycle (Thomas et al. 2009; Deschamps et al. 2012). More specifically, this new data set encompasses the part of the last deglaciation that was marked by the transition between Heinrich event 1 and the Bølling warming that was synchronous with the Melt Water Pulse 1A (MWP-1A) event, a dramatic ice-sheet collapse that occurred 14.65 kyr BP ago. This rapid sea-level rise of about 14 m in less than 350 yr (Deschamps et al. 2012) very probably disturbed oceanic thermohaline circulation (McManus et al. 2004) and consequently ocean ventilation. The sequence of abrupt climatic events, i.e. the Bølling warming and the MWP-1A event, that punctuated this time interval, included perturbations of the global carbon cycle, marked by the increase of atmospheric CO_2 (Lourantou et al. 2010) or variations in the $\Delta^{14}C$ records (Reimer et al. 2009). Establishing an absolute and accurate chronological framework of the different climatic archives (marine, continental, ice) that cover this key period of the last deglaciation is thus pivotal for understanding the temporal and causal relationship between theses abrupt climatic events. However, this requires a calibration of the ^{14}C scale because most of these archives are ^{14}C dated. As pointed out by the IntCal Working Group (Stuiver et al. 1998; Hughen et al. 2004c; Reimer et al. 2004, 2009), some questions related to the resolution and accuracy of the calibration curve remain unresolved for this period. Indeed, for the onset of the deglaciation period, from 17.5 to 14 cal kyr BP, there are important discrepancies between the different marine sediment records, i.e. between the Iberian Margin record and the Cariaco Basin record, and also between the Cariaco Basin record and the coral data sets (Reimer et al. 2009). The inconsistency of these records within this interval may ultimately reflect changes in pool-to-pool ^{14}C gradients and therefore may provide valuable insights into ocean ventilation and carbon cycle dynamics. In this paper, we will discuss the implications of the new Tahiti data set for the calibration of the ^{14}C timescale for the crucial 14–17.5 cal kyr BP period, as well as its implication for constraining past variation of marine reservoir ages.

MATERIAL AND METHODS

Sites and Samples

The IODP "Tahiti Sea Level" Expedition (IODP 310) (October–November 2005) recovered coral samples from submerged fossil reefs at 3 different locations around Tahiti Island (Faaa, Tiarei, and Maraa, Figure 1). A total of 37 boreholes were drilled at 22 different sites at water depths ranging from 41.6 to 117.5 m. More than 600 m of reef cores were retrieved from 41.6 to 161.8 m below sea level, with an exceptional recovery (>90% of carbonate rocks) and well-preserved original coral frameworks (Camoin et al. 2007a,b). Preservation of the primary reef framework was enhanced by the rapid colonization of encrusting algae and microbialithe shortly after the corals died. These organisms also potentially "shielded" the corals from diagenetic alteration. The reef sequences cover most of the last deglaciation period. Various species of corals (mainly *Porites* and *Pocillopora* sp.) were selected and dated in 22 different holes from 13 sites (Figure 1). The collected coral material provides a continuous and detailed record of sea-level rise during the key period encompassing the MWP-1A event and demonstrates that this rapid collapse of former ice sheets was synchronous with the Bølling warming (Deschamps et al. 2012). Material older than the Last Glacial Maximum was also recovered at each of the 3 locations (Camoin et al. 2007a,b) and several cores contained pre-LGM corals suitable for U-Th dating (Thomas et al. 2009), including well-preserved samples from marine isotope stage 3.
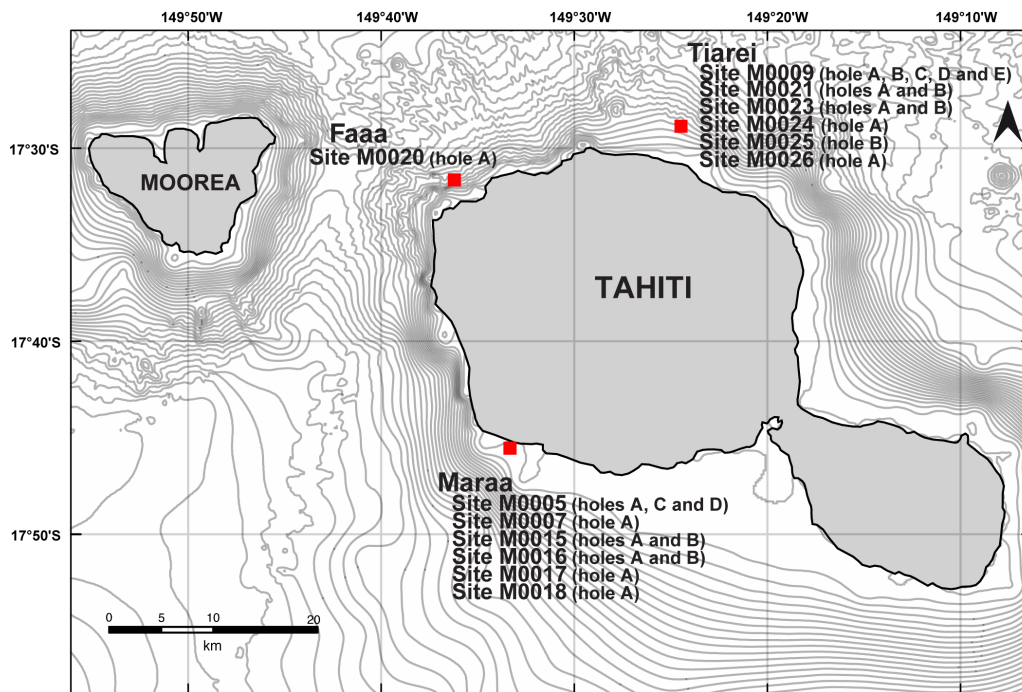

Figure 1 Map of Tahiti showing the locations of the 3 areas (Maraa, Faaa, and Tiarei) investigated during the IODP Expedition 310 operations (red squares) (from Camoin et al. 2007a,b). Only the drill sites that have been sampled for this study are shown, with their associated boreholes.

X-Ray Diffraction

Before ^{14}C and U-Th analyses, powder X-ray diffraction (XRD) analyses were performed for each coral sample, in order to select pristine aragonitic coral skeletons and avoid those containing diagenetic calcite that may alter original ages. We used a calibration method optimized for the detection and quantification of very low amounts of secondary calcite. The procedure, implemented at CEREGE, is described in detail in Sepulcre et al. (2009). An aragonite-calcite calibration curve was assessed on 2 different XRD instruments at CEREGE (Philips PW 3710 and Philips X'PERT PRO), by means of 19 gravimetric standard mixtures containing 0.3 to 95% pure calcite. A Mg-calcite/calcite calibration was also performed using 10 standards between 5% and 90% calcite. The XRD peak areas were used for precise quantification of low amounts of calcite (<3%) rather than peak heights alone, as the best reproducibility was obtained with the peak area ratios. Indeed, a calibration based on peak heights may underestimate the calcite content because of the occurrence of Mg-calcite in some altered corals. Moreover, the secondary calcite can be a mixture of Mg-rich and Mg-poor calcite, leading to a flattened calcite peak with a very low height/area ratio, much broader than for pure calcite (Reimer et al. 2006). In order to take into account the heterogeneity of natural samples, XRD measurements were carried out on 3 distinct slides for each sample. The detection limit achieved with this method is 0.2% calcite in a calcite-aragonite mixture (Sepulcre et al. 2009). The Tahiti coral samples were analyzed with the Philips X'PERT PRO diffractometer (Cobalt Kα tube, 40kV/40mA, Step 0.05°, time per step 10 s), which features a fixed sample, with source and detector spinning around it. XRD data were processed with the PC-APD software (Analytical Powder Diffraction, v 3.6, Philips Electronics). As discussed below, only samples that passed the "1% calcite" criterion were considered for calibration purposes (Stuiver et al. 1998; Hughen et al. 2004c; Reimer et al. 2006, 2009).

U-Th Dating of Corals

About 2 g of coral samples were spiked with a mixed ^{233}U-^{236}U-^{229}Th solution, before being totally dissolved in nitric acid (for details on the preparation and calibration of the spike solution, see Deschamps et al. 2012). Chemical separation and further purification of U and Th fractions from the sample matrix followed the procedure described previously (Edwards et al. 1987b; Bard et al. 1990c, 1996): U and Th were coprecipitated with iron hydroxide by adding ammonium hydroxide, then separated and purified by successive steps on AG1-X8 anionic resin, and a last step for U on UTEVA resin. Total procedural blanks were between 11 and 44 pg for Th (mean value of 30 pg, $n = 9$) and between 17 and 65 pg for U (mean value of 40, $n = 9$). The U-Th analyses were performed at CEREGE using a VG-54 thermal ionization mass spectrometer equipped with a 30-cm electrostatic analyzer and an ion-counting Daly detector.

For U analyses, masses 233, 234, 235, and 236 were measured in peak jumping mode on the Daly detector. The ^{236}U/^{233}U ratio was used to monitor internally the instrumental mass bias. This strategy avoids monitoring the large ^{238}U ion beam, and obviates many of the problems related to gain calibration of the Daly/Faraday detectors (Deschamps et al. 2003; Stirling et al. 2007). For Th analyses, the techniques used were similar to those reported previously (Bard et al. 1990c, 1996). For consistency with previously published data sets, ^{234}U/^{238}U and ^{230}Th/^{238}U were computed using the conventional reference value of 137.88 for the natural ^{238}U/^{235}U ratio (Cowan and Adler 1976; Cheng et al. 2000). Recent measurements have demonstrated natural variability in this ratio (Stirling et al. 2007; Weyer et al. 2008). In particular, a value of $137.769 \pm 0.011/0.024$ was reported recently by Condon et al. (2010) in HU-1. However, this difference of <1‰ with the conventional ^{238}U/^{235}U value leads to an insignificant change in final calculated ages (Deschamps et al. 2012).

The analytical reproducibility achieved in the course of this study was assessed by replicate measurements of the NBS-960 standard, and yielded a mean value of $\delta^{234}U = -36.5 \pm 0.8‰$ (2σ, $n = 23$), in excellent agreement with previous measurements at CEREGE ($\delta^{234}U = -36.6 \pm 3.7‰$ [2σ, $n = 6$; Bard et al. 1996] and $\delta^{234}U = -37.6 \pm 1.9‰$ [2σ, $n = 23$, Delanghe et al. 2002]), and with values reported in the literature (Andersen et al. 2004; Deschamps et al. 2003). Internal reproducibility was also checked by replicate U-Th measurements of several samples that all showed agreement within errors. U-Th measurements were also duplicated on several samples in parallel by the Oxford (see Thomas et al. 2009 and Mason and Henderson 2010 for an overview of methods) and CEREGE teams, which again showed agreement within error (Deschamps et al. 2012). U-Th ages are presented in years before AD 1950, with 2σ error. The precision of ^{230}Th/U ages generally falls within the 1.5–4‰ range (i.e. ±20–50 yr in ages in the case of postglacial samples).

^{14}C Analyses

^{14}C analyses were performed by accelerator mass spectrometry (AMS) at the ARTEMIS National Facility installed at Saclay, France (Cottereau et al. 2007; Moreau et al. 2013). Coral samples were hand-picked as millimetric grains selected randomly within the same batch used for U-Th analyses. The coral samples were cleaned by acid leaching to remove surface contamination, leading to 30% to 50% weight loss (Bard et al. 1990c). The aim of this leaching is to remove material probably made of recrystallized phases and to avoid potential contamination by modern carbon prior to ^{14}C isotopic analyses. Large carbonate subsamples (10–14 mg) were then converted to CO_2 to obtain around 1 mg of C. The CO_2 extracted from samples is reduced to graphite, using iron powder as a catalyst in the presence of an excess of hydrogen (Vogel et al. 1984), in order to produce the accelerator targets (Cottereau et al. 2007).

^{14}C ages were calculated according to Mook and van der Plicht (1999), by correcting for fractionation with the ^{13}C/^{12}C ratio measured on ARTEMIS. The average machine blank obtained on pure graphite is 0.015 ± 0.008 pMC (percent modern carbon) (1σ, $n = 168$), which corresponds to an age of 71.7 ± 4.1 kyr BP. The background correction is based on measurements of an internal standard made from a fossil *Tridacna* shell (older than 50,000 yr) that yields a value of 0.116 ± 0.038 pMC (1σ, $n = 60$), corresponding to an age of 54.7 ± 2.6 kyr BP. Note that the uncertainty of this value is propagated in the error calculation on the ages.

Duplicate analyses were performed on 15 coral samples from different time windows: 1 sample at ~10.5 kyr BP; 13 between 12 and 13.5 kyr BP; and 1 sample at 25 kyr BP (Figure 2). All these replicated ages agree with each other within their 2σ uncertainties. In order to further check the reproducibility, 1 sample was also analyzed 5 times (Figure 2); results were again consistent within error. Replicate analyses were also performed for 5 samples at the MALT facility (Micro Analysis Laboratory, Tandem accelerator), University of Tokyo (Figure 3A). For 3 samples, stepwise dissolution measurements were done following procedures described by Yokoyama et al. (2000, 2007) and Yokoyama and Esat (2004) in order to check the efficiency of the chemical pretreatment. Measurements on the successive dissolution steps exhibit similar ages only after at least 10% of the sample has been leached away (Figure 3B). This pretreatment removes a contamination corresponding to ~0.2 to 3% of the total pMC value. The ages obtained during these tests are in good agreement with each other, supporting the efficiency of the pretreatments applied in both laboratories (Figure 3B). ^{14}C ages are reported prior to AD 1950. We use the same correction of 300 yr for the site-specific reservoir age at Tahiti as Bard et al. (1998).
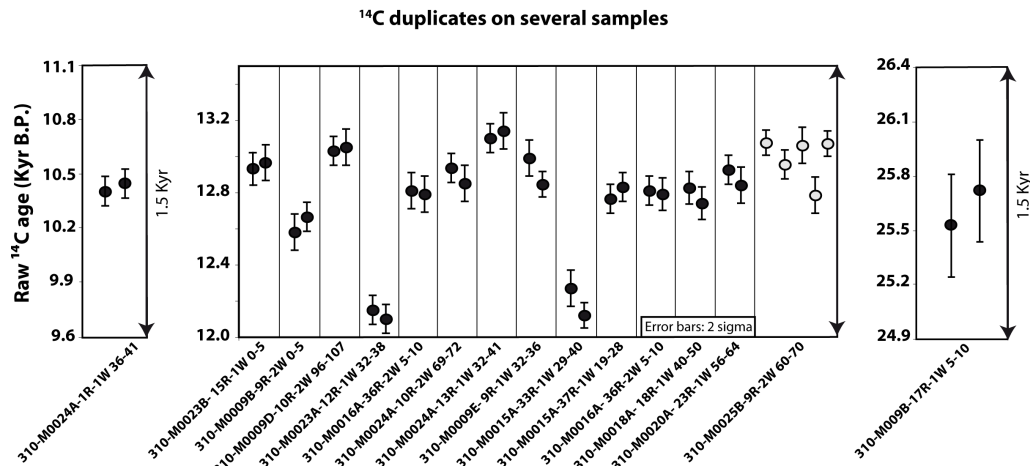
¹⁴C duplicates on several samples

Figure 2 Replicated ¹⁴C analysis for different time windows of 16 coral samples from Tahiti offshore barrier reef. The gray circles correspond to the results for the sample measured 5 times. The double arrows indicate the same range of 1.5 kyr for the 3 panels. Measurements were performed by AMS at the National Facility ARTEMIS at the LMC14 Laboratory, Gif-sur-Yvette, France.

RESULTS

A total of 77 coral samples were cross-dated by U-Th and ¹⁴C (Tables 1 and 2). The calendar ages of the corals range from 10 to 36 cal kyr BP, including 70 dates for the deglaciation period, and 7 glacial samples with ages from 29 to 37 cal kyr BP. The new data obtained from the IODP 310 expedition extend the previous Tahiti record, based on cores drilled onshore on the modern Tahiti barrier reef, which was limited to the last 13.9 cal kyr BP (Bard et al. 1998, 2010). The new results are first presented and assessed in light of the different mineralogical and geochemical screening criteria, in order to check the validity of the coral ages. Then, the samples that passed all the screening criteria are compared to the IntCal data sets used for calibration of the ¹⁴C timescale for the last deglacial period.

U-Th and ¹⁴C Analyses: Screening Criteria

In order to detect possible postdepositional diagenesis in our samples, we used successively the screening criteria recommended by the IntCal Working Group (Reimer et al. 2002, 2009; Hughen et al. 2004c): calcite content; U and Th concentrations; and initial $(^{234}U/^{238}U)_0$ values. The selection of the samples according to the screening criteria is discussed below.

Calcite Content of the Coral Samples

As recommended by the IntCal group, samples that passed the test of <1% calcite were dated by U-Th. As an additional test, 7 post-glacial samples showing calcite content >1% were also cross-dated by U-Th and ¹⁴C for comparison purposes (Table 2). There is no significant difference between the ages of contaminated samples and the closest sample free of calcite (<1%) (within the error bars) (Figure 4). This suggests that the calcite alteration occurred shortly after the coral death and therefore will have little impact on the age determinations. This suggests that in the case of the Tahiti corals, the tiny amounts of calcite in the <1% samples will have no impact on the ages. There is no obvious systematic correlation between the calcite content and the U concentration and/or the $\delta^{234}U$ (Figure 5A). Note that the 7 samples older than 29 cal kyr BP have <1% calcite.

Table 1 U, Th, and 14C analytical results processed at the ARTEMIS lab.

Sample	Calcite (%)	232Th (ppb)	238U (ppb)	$(^{234}U/^{238}U)_0$ ±2σ	U-Th lab[a]	U-Th age (yr BP) ±2σ	14C age[b] (yr BP) ±2σ	Δ14C ±2σ
310-M007A-18R-1W 76-90	0.6	0.57	2751	1.1474 ± 0.0006	CE	10,029 ± 18	8875 ± 60	114 ± 9
310-M005A-12R-1W 51-54	0.7	0.15	2403	1.1468 ± 0.0005	CE	11,033 ± 15	9585 ± 70	152 ± 10
310-M0018A-7R-1W 73-82	0.2	0.65	3321	1.1477 ± 0.0005	CE	11,488 ± 29	9980 ± 70	159 ± 11
310-M005C-11R-1W 46-59	0.0	0.04	3468	1.1466 ± 0.0003	CE/OX	11,837 ± 14*	10,070 ± 70	195 ± 11
310-M0023A-5R-1W 45-52	0.2	0.30	2360	1.1477 ± 0.0007	CE	12,370 ± 36	10,395 ± 70	224 ± 12
310-M005D-2R-1W 107-115	0.0	0.79	2623	1.1470 ± 0.0005	CE	12,430 ± 27	10,480 ± 70	220 ± 11
310-M005D-5R-2W 0-5	0.2	0.18	2736	1.1470 ± 0.0010	CE	13,163 ± 44	11,245 ± 70	212 ± 12
310-M0023A-11R-1W 22-31	0.2	1.30	2985	1.1463 ± 0.0008	CE	13,460 ± 21	11,630 ± 80	198 ± 12
310-M0015A-33R-1W 29-40	0.0	0.21	2835	1.1460 ± 0.0005	CE	13,577 ± 23*	11,869 ± 57*	179 ± 9
310-M0023A-12R-1W 32-38	0.2	2.23	2924	1.1458 ± 0.0005	CE	13,580 ± 21	11,825 ± 57*	186 ± 9
310-M0020A-16R-1W 55-66	0.3	1.77	3190	1.1471 ± 0.0019	OX	13,724 ± 57	11,695 ± 80	227 ± 15
310-M0023A-12R-1W 140-144	0.6	2.67	2581	1.1459 ± 0.0005	CE	13,736 ± 18	12,190 ± 80	155 ± 12
310-M005D-6R-2W 0-5	0.2	0.62	3558	1.1459 ± 0.0008	CE	13,784 ± 31	11,930 ± 80	200 ± 13
310-M009C-6R-1W 38-43	0.2	0.85	2815	1.1465 ± 0.0007	CE	13,848 ± 29	12,000 ± 100	199 ± 16
310-M0023B-12R-1W 30-33	0.0	1.71	3722	1.1454 ± 0.0006	CE	13,988 ± 16	12,275 ± 70	178 ± 11
310-M0021A-13R-2W 66-75	0.2	0.48	2429	1.1452 ± 0.0004	CE	14,015 ± 27*	12,020 ± 100	220 ± 16
310-M009E-7R-1W 5-13	0.2	0.44	2539	1.1456 ± 0.0005	CE	14,116 ± 43	12,285 ± 100	195 ± 16
310-M0020A-21R-2W 13-20	0.0	0.46	2984	1.1471 ± 0.0006	CE	14,145 ± 45	12,230 ± 80	208 ± 14
310-M009D-7R-1W 11-28	0.2	0.26	2594	1.1459 ± 0.0007	CE	14,221 ± 56	12,380 ± 80	196 ± 14
310-M009A-6R-1W 38-48	0.2	1.80	3589	1.1447 ± 0.0009	OX	14,239 ± 33	12,250 ± 120	218 ± 19
310-M0018A-18R-1W 40-50	0.2	0.13	2405	1.1465 ± 0.0007	CE	14,273 ± 63	12,483 ± 64*	188 ± 13
310-M0023B-12R-2W 113-127	0.5	0.46	2707	1.1453 ± 0.0004	CE	14,278 ± 15*	12,500 ± 71*	187 ± 11
310-M0023B-15R-1W 0-5	0.2	1.53	2663	1.1455 ± 0.0004	CE	14,284 ± 27	12,639 ± 77*	167 ± 12
310-M0023A-13R-2W 32-37	0.0	0.46	2667	1.1462 ± 0.0005	CE	14,312 ± 38	12,585 ± 100	179 ± 16
310-M0018A-19R-1W 107-110	0.2	0.68	2576	1.1451 ± 0.0006	CE	14,338 ± 27	12,545 ± 80	189 ± 12
310-M009B-9R-2W 0-5	0.2	0.71	3009	1.1456 ± 0.0004	CE	14,348 ± 22*	12,332 ± 62*	222 ± 10
310-M0021B-16R-1W 39-44	0.2	0.49	3060	1.1454 ± 0.0005	CE	14,350 ± 22	12,675 ± 100	171 ± 15
310-M009E-9R-1W 32-36	0.3	0.43	2456	1.1453 ± 0.0009	OX	14,359 ± 39	12,545 ± 80	192 ± 13
310-M0015A-36R-1W 51-52	0.2	1.08	3641	1.1455 ± 0.0005	CE	14,418 ± 26	12,625 ± 90	188 ± 14
310-M0020A-23R-1W 56-64	0.15	0.17	2836	1.1459 ± 0.0008	CE	14,456 ± 59	12,592 ± 62*	199 ± 13
310-M0025A-10R-1W 40-46	0.5	1.52	2771	1.1451 ± 0.0005	CE	14,478 ± 24	12,593 ± 57*	202 ± 9
310-M009D-9R-1W 66-77	0.2	1.65	3047	1.1452 ± 0.0005	CE	14,490 ± 33	12,540 ± 100	211 ± 16
310-M0015A-36R-2W 0-6	0.2	0.80	3739	1.1452 ± 0.0006	CE	14,516 ± 19	12,615 ± 100	204 ± 15

Table 1 U, Th, and ^{14}C analytical results processed at the ARTEMIS lab. *(Continued)*

Sample	Calcite (%)	^{232}Th (ppb)	^{238}U (ppb)	$(^{234}U/^{238}U)_0$ ±2σ	U-Th lab[a]	U-Th age (yr BP) ±2σ	^{14}C age[b] (yr BP) ±2σ	Δ^{14}C ±2σ
310-M009B-13R-1W 11-18	0.2	1.7	3291	1.1451 ± 0.0005	CE	14,519 ± 20	12,630 ± 100	202 ± 15
310-M009D-9R-1W 99-103	0.3	0.95	3046	1.1452 ± 0.0004	CE	14,531 ± 45	12,650 ±	201 ± 15
310-M0016A-36R-2W 5-10	0.0	0.16	2553	1.1455 ± 0.0006	CE	14,555 ± 24	12,501 ± 60*	227 ± 10
310-M0024A-10R-1W 65-75	0.7	0.20	2727	1.1451 ± 0.0010	CE	14,582 ± 52	12,430 ± 100	242 ± 17
310-M0023A-14R-1W 0-20	0.2	1.30	2651	1.1461 ± 0.0006	CE	14,588 ± 25	12,450 ± 80	240 ± 13
310-M0024A-10R-1W 98-116	0.6	1.18	2620	1.1452 ± 0.0005	CE	14,609 ± 26	12,620 ± 140	217 ± 22
310-M0015A-37R-1W 19-28	0.0	0.28	3503	1.1451 ± 0.0007	CE	14,650 ± 22	12,498 ± 57*	242 ± 9
310-M0020A-24R-2W 38-42	0.1	0.56	3193	1.1418 ± 0.0019	OX	14,663 ± 61	12,355 ± 80	266 ± 16
310-M0026A-5R-1W 4-18	0.2	0.33	2517	1.1451 ± 0.0006	CE	14,720 ± 25	12,635 ± 90	231 ± 14
310-M0020A-23R-2W 72-78	0.3	0.27	2869	1.1446 ± 0.0009	OX	14,734 ± 57	12,515 ± 100	252 ± 18
310-M0024A-10R-2W 69-72	0.0	0.99	2833	1.1447 ± 0.0005	CE	14,748 ± 25	12,602 ± 62*	240 ± 10
310-M009E-9R-1W 69-73	0.1	0.63	2799	1.1427 ± 0.0009	OX	14,769 ± 37	12,475 ± 80	263 ± 14
310-M009D-10R-2W 96-107	0.0	0.61	2523	1.1433 ± 0.0014	CE/OX	14,793 ± 26*	12,738 ± 62*	226 ± 10
310-M0025B-9R-2W 60-70	0.2	0.30	2522	1.1448 ± 0.0006	CE	14,801 ± 32	12,709 ± 36*	232 ± 7
310-M0026A-5R-1W 117-127	0.5	0.52	2731	1.1448 ± 0.0006	CE	14,853 ± 30	12,780 ± 160	228 ± 25
310-M0025B-10R-1W 0-5	0.2	0.29	2493	1.1454 ± 0.0005	CE	14,901 ± 22	12,610 ± 120	262 ± 19
310-M009D-11R-1W 13-20	0.0	2.93	2600	1.1435 ± 0.0014	CE/OX	14,912 ± 26*	12,685 ± 80	252 ± 13
310-M0024A-11R-2W 23-38	0.7	0.42	2555	1.1453 ± 0.0004	CE	14,994 ± 25*	12,725 ± 80	258 ± 13
310-M009B-14R-1W 22-25	0.2	2.5	3138	1.1423 ± 0.0009	CE	15,146 ± 24	12,860 ± 100	260 ± 16
310-M0024A-13R-1W 32-41	0.0	0.58	2701	1.1454 ± 0.0007	CE	15,147 ± 31	12,816 ± 62*	267 ± 11
310-M0024A-14R-1W 24-28	0.5	0.12	2393	1.1453 ± 0.0005	CE	15,232 ± 33*	13,085 ± 90	238 ± 15
310-M0025B-11R-1W 70-74	0.2	0.82	2689	1.1453 ± 0.0008	CE	15,310 ± 23	13,110 ± 120	246 ± 19
310-M009C-17R-2W 0-10	0.0	0.80	2616	1.1453 ± 0.0008	CE	15,512 ± 27	13,310 ± 100	245 ± 16
310-M0024A-15R-1W 16-20	0.2	2.15	3002	1.1452 ± 0.0005	CE	15,744 ± 29	13,400 ± 80	267 ± 13
310-M009B-15R-1W 13-20	0.2	0.37	2937	1.1445 ± 0.0013	CE/OX	16,087 ± 42*	13,580 ± 100	291 ± 17
310-M009D-14R-2W 81-90	0.3	1.54	4075	1.1387 ± 0.001	CE	29,209 ± 51	25,230 ± 220	481 ± 42
310-M009B-16R-2W 13-17	0.2	0.38	3262	1.1380 ± 0.001	OX	29,631 ± 62*	25,670 ± 200	475 ± 38
310-M009B-17R-1W 70-80	0.1	0.707	3557	1.1420 ± 0.001	OX	29,666 ± 58*	24,960 ± 200	618 ± 42
310-M009B-17R-1W 5-10	0.5	0.354	3479	1.1410 ± 0.001	OX	29,838 ± 53*	25,325 ± 198*	579 ± 40
310-M009D-18R-1W 19-28	0.2	1.623	4079	1.1390 ± 0.001	OX	30,195 ± 55*	25,750 ± 200	564 ± 40
310-M009D-20R-2W 0-5	0.5	1.472	3255	1.1440 ± 0.001	OX	30,991 ± 56	25,130 ± 100	860 ± 26
310-M0025A-11R-1W 58-68	0.2	0.19	3770	1.1486 ± 0.001	CE	36,326 ± 83	31,910 ± 440	525 ± 85

[a]CE: CEREGE; OX: Oxford.

[b]^{14}C ages are conventional ages with a reservoir correction of 300 yr. All ^{14}C measurements were performed at the ARTEMIS lab.

*Reported ^{14}C and U-Th age is the weighted mean of 2 or more replicates (see Deschamps et al. 2012 and Thomas et al. 2009 for U-Th ages).
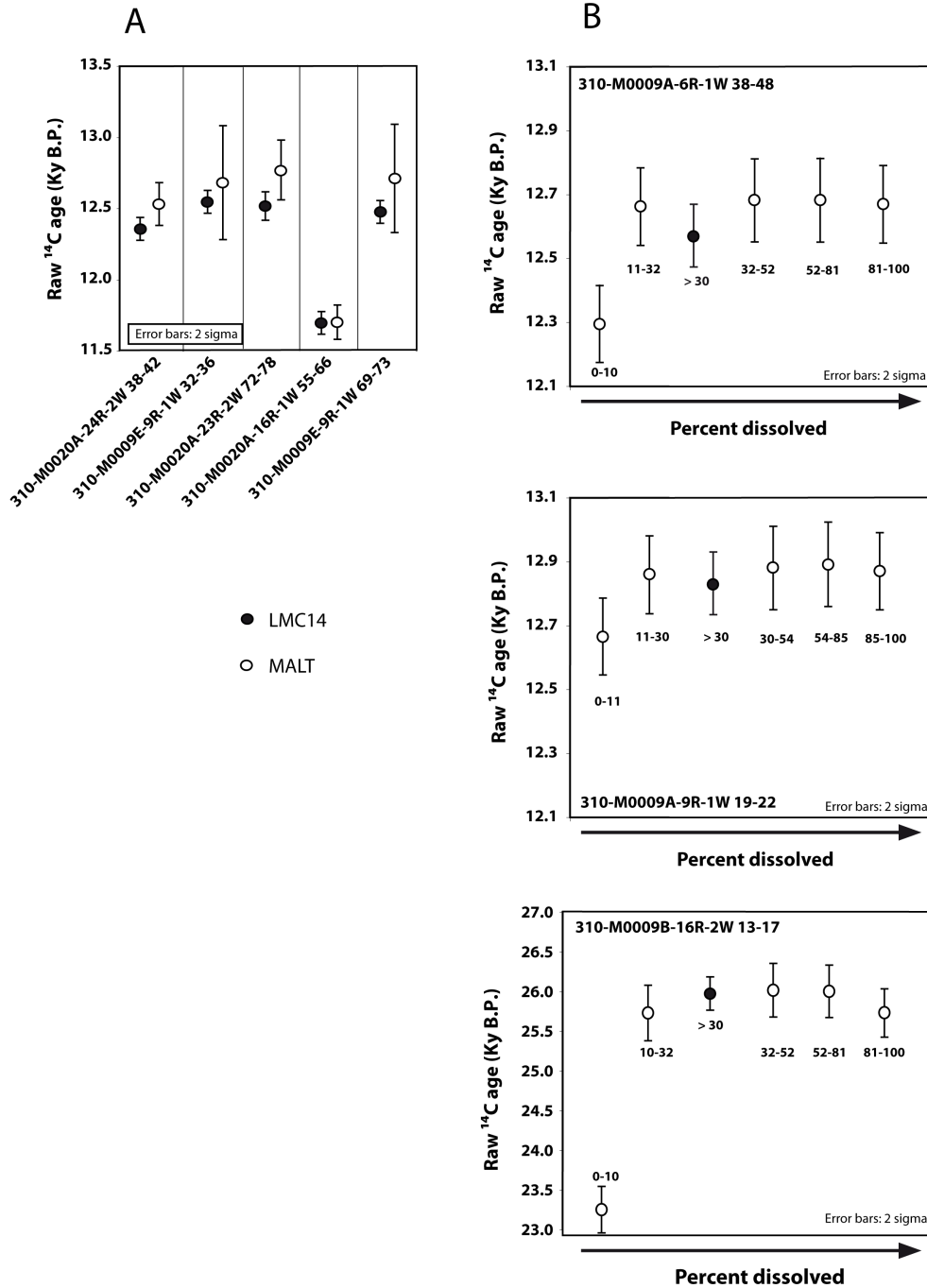
Figure 3 A) Replicated 14C analysis for 5 coral samples performed at the MALT (Micro Analysis Laboratory, Tandem accelerator, University of Tokyo, Japan) (open circles) and at the LMC14 (black circles). B) Comparison between stepwise dissolution measurements at the MALT (open circles) and measurement after chemical pretreatment with acid leaching (>30% weight loss of the total weight) at the LMC14 (black circles), performed on 3 samples of different ages.

Table 2 U, Th, and ^{14}C analytical results of samples that were discarded.

Sample	Calcite (%)	^{232}Th (ppb)	^{238}U (ppb)	$(^{234}U/^{238}U)_0$ ±2σ	U-Th lab[a]	U-Th age (yr BP) ±2σ	^{14}C age[b] (yr BP)
310-M0023A-11R-2W 112-121	0.2	3.63	2513	1.1469 ± 0.0005	CE	13,569 ± 23	11,735 ± 100
310-M009A-9R-1W 19-22	0.2	3.20	3589	1.1439 ± 0.0009	OX	14,374 ± 33	12,525 ± 100
310-M0021A-17R-1W 13-19	0.2	5.56	3799	1.1443 ± 0.0010	CE	14,332 ± 41	12,495 ± 100
310-M0024A-1R-1W 36-41	0.5	7.36	4119	1.1468 ± 0.0006	CE	12,315 ± 34*	10,122.5 ± 57
310-M0024A-4R-1W 137-141	0.7	10.61	2849	1.1475 ± 0.0006	CE	13,561 ± 40	11,560 ± 80
310-M0023A-6R-1W 8-15	16.8	0.43	2732	1.1473 ± 0.0006	CE	12,404 ± 49	10,440 ± 70
310-M0017A-19R-1W 72-86	7.2	0.14	2700	1.1463 ± 0.0006	CE	12,875 ± 30	10,860 ± 70
310-M0015B-37R-1W 57-63	7.1	0.19	2732	1.1472 ± 0.0053	CE	13,799 ± 77	12,130 ± 80
310-M009D-7R-1W 28-45	1.1	0.21	2604	1.1452 ± 0.0009	CE/ OX	14,222 ± 18*	12,400 ± 100
310-M0023B-15R-1W 0-5	4.8	0.76	3109	1.1447 ± 0.0004	CE	14,469 ± 23	12,640 ± 100
310-M0018A-22R-1W 2-12	2.2	0.04	2584	1.1441 ± 0.0046	OX	14,784 ± 74	12,740 ± 80
310-M0024A-12R-2W 133-136	2.1	0.45	2667	1.1449 ± 0.0006	CE	15,236 ± 51	12,815 ± 90

[a]CE: CEREGE; OX: Oxford.

[b]^{14}C ages are conventional ages with a reservoir correction of 300 yr. All ^{14}C measurements were performed at the ARTEMIS lab.

*Reported U-Th age is the weighted mean of 2 or more replicates (see Deschamps et al. 2012 for U-Th ages).
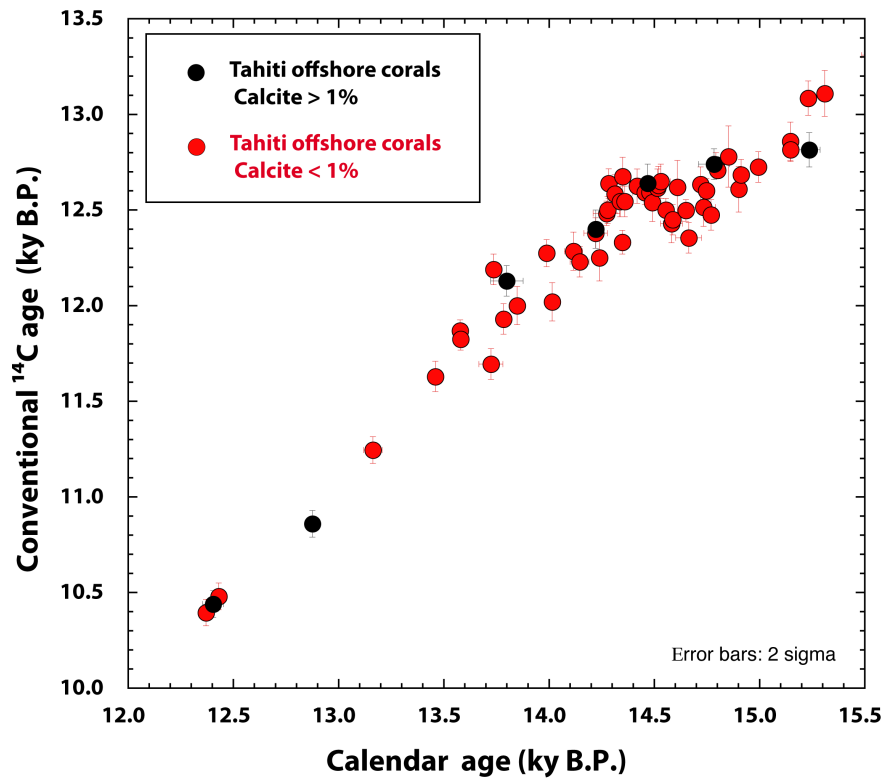

Figure 4 ^{14}C ages plotted versus calendar ages of Tahiti samples with calcite content <1% (red circles) and Tahiti samples with calcite content >1% (black circles). Note that samples with >1% of calcite are in good agreement (within the error bars) with the calcite-free sample (<1%) ^{14}C ages are conventional ages in kyr BP corrected from the reservoir age. Tahiti data (red circles) have been corrected from a reservoir age of 300 yr (Bard et al. 1998).
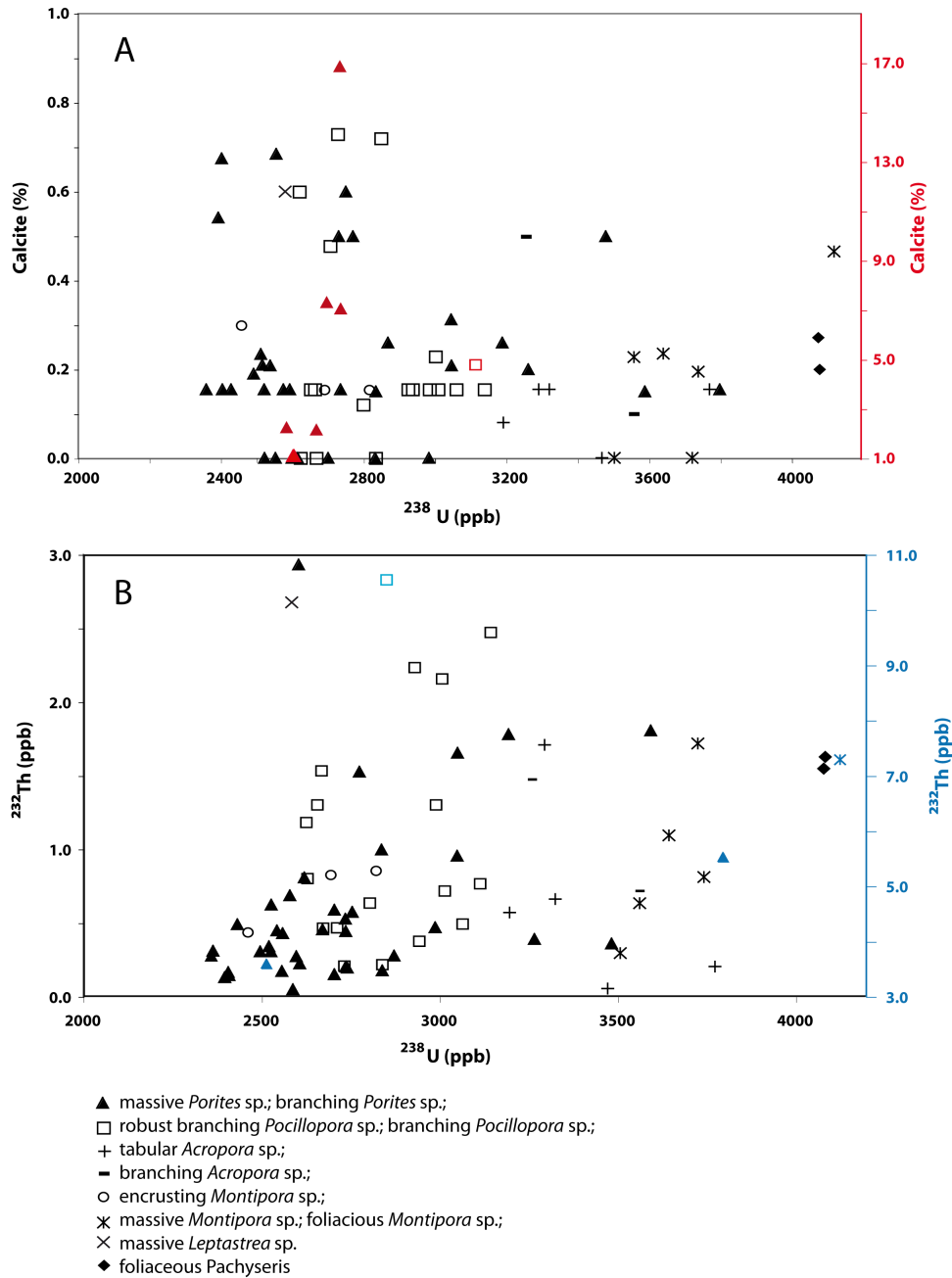
Figure 5 A) Relationship between the calcite content and the U concentration in Tahiti coral samples. The left *y* axis is for low-calcite samples (<1%, black symbols) and the right *y* axis is for high-calcite samples (>1%, red symbols). Note that the *y* axes use different values and amplitudes for calcite content. Overall, there is no obvious correlation between the calcite content and the U concentration. B) Relationship between the ^{232}Th content and the U concentration in Tahiti coral samples. Left *y* axis is for low ^{232}Th samples (<3 ppb, black symbols) and right axis is dedicated to high values (>3 ppb, blue symbols). Note that the *y* axes use different values and amplitudes for ^{232}Th content. Overall, there is no obvious systematic correlation between ^{232}Th content and the U concentration. Samples with ^{232}Th >3 ppb were discarded (see text). Different symbols are used to indicate the various coral species.

U and Th Concentration

The U concentration of Tahiti offshore corals range between ~2.3 and 4.1 ppm (Table 1). These values are within the expected range for modern corals considering the species dependence of uranium content (e.g. Zhu et al. 1993) and the sea surface temperature dependence (Min et al. 1995; Cardinal et al. 2001). Indeed, the highest U contents (3.3–4.1 ppm) in this study are measured mostly in *Montipora* and *Acropora* species, in good agreement with previous work (Stirling et al. 1995; Min et al. 1995) (Figures 5A and B).

^{232}Th is typically <1 ppb in modern corals (Edwards et al. 1987a; Chen et al. 1991). ^{232}Th in excess of this value may be indicate the presence of detrital ^{230}Th, potentially inducing bias on the measured U-Th ages. In this study, Th concentrations are <1 ppb for 54 samples (including the samples with calcite content >1%), and between 1 and 7 ppb for 22 others. Only 1 sample reaches 10 ppb (Tables 1 and 2).

These higher ^{232}Th values could be related to the occurrence of microbialithes in the Tahiti reef sequences. Indeed, most of the samples with ^{232}Th >1 ppb are from the Tiarei site (except 2 samples from the Faaa site), where microbialithes may account for as much as 80% of the carbonate sequence (Seard et al. 2011). In any case, there is again no correlation between the ^{232}Th content and uranium concentration. Moreover, most samples with ^{232}Th >1 ppb appeared in good agreement with the other samples in terms of ^{14}C and U-Th ages. As a conservative precaution, we discarded 5 samples with ^{232}Th >3 ppb. The samples older than 20 cal kyr BP have Th concentrations <1 ppb except for 2 samples (1.62 and 1.47 ppb).

Initial (^{234}U/^{238}U)$_0$

The initial (^{234}U/^{238}U)$_0$ values calculated for our deglacial samples yielded a mean value of 1.1454 ± 0.002 (2σ, $n = 58$), falling within the most recent determinations of modern seawater and corals (Delanghe et al. 2002; Cutler et al. 2004; Robinson et al. 2004) and in good agreement with the (^{234}U/^{238}U)$_0$ values obtained on corals drilled onshore Tahiti (Bard et al. 1996, 2010) (Figure 6). It is noteworthy that the (^{234}U/^{238}U)$_0$ measurements in our samples exhibit a smaller range of variation than the range fixed by the IntCal group (Reimer et al. 2009) as a screening criteria for corals younger than 17 kyr [(^{234}U/^{238}U))$_0$ = 1.147 ± 0.007, 3σ]. Indeed, our data are all consistent within the analytical reproducibility achieved in the course of the study (0.8‰, 2σ, $n = 23$), while previous data sets for the same period (Vanuatu, Papua New Guinea, and Barbados; Cabioch et al. 2003; Cutler et al. 2004; Fairbanks et al. 2005) generally showed (^{234}U/^{238}U)$_0$ variations larger than the analytical reproducibility (Figure 6).

The initial (^{234}U/^{238}U)$_0$ values calculated for the samples older than 20 cal kyr BP yielded a mean value of 1.1416 ± 0.0075 (2σ, $n = 7$), in agreement with the range adopted by Reimer et al. (2009) for samples older than 17 kyr BP [(^{234}U/^{238}U)$_0$ = 1.1417 ± 0.0078, 3σ]. Therefore, our results confirm that coral samples older than 20 kyr BP tend to have lower ^{234}U$_{initial}$ values than deglacial samples, probably reflecting real variability of past seawater ^{234}U/^{238}U ratios with time (Robinson et al. 2004; Esat and Yokoyama 2006). In sum, after discarding 12 samples considering these various screening criteria, we retain 58 samples for the 10–16 cal kyr BP deglaciation period, with a higher resolution (33 data) for the 14.2–15.0 cal kyr BP time interval. The 7 samples older than 20 cal kyr BP all passed the screening tests.
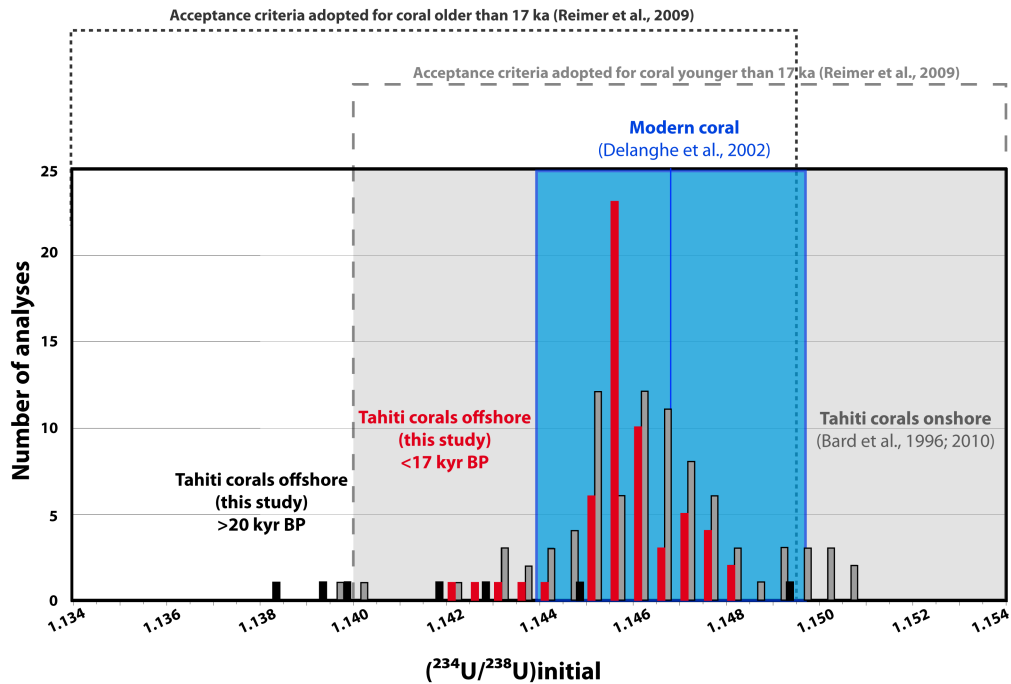
Figure 6 Repartition of the initial $(^{234}U/^{238}U)_0$ values calculated for deglacial Tahiti coral samples younger than 17 kyr (red bars) (mean value of 1.1454 ± 0.002, 2σ, n = 58) and older than 20 kyr (black bars) (mean value of 1.1416 ± 0.0075, 2σ, n = 7). The gray area marks the initial $(^{234}U/^{238}U)_0$ ratio screening criteria for coral younger than 17 kyr (1.147 ± 0.007, 3σ, Reimer et al. 2009). The average value measured in modern corals by Delanghe et al. (2002) (1.1466 ± 0.0028) is also reported (blue line with its 2σ envelope). The $(^{234}U/^{238}U)_0$ values obtained from the corals drilled offshore are also compared to the $(^{234}U/^{238}U)_0$ values obtained from corals drilled onshore Tahiti (Bard et al. 1996, 2010) (gray bars).

Comparison with Previous Data Sets

Figure 7 illustrates the comparison between the new results from Tahiti and the different types of data sets used in the IntCal04 and IntCal09 ^{14}C calibrations (Reimer et al. 2004, 2009), for the period from 10 to 18 cal kyr BP corresponding to the last deglaciation. The coral data are shown in Figure 7A, including samples from Araki, Barbados, and Kirimati (Fairbanks et al. 2005); Vanuatu and Papua New Guinea (Cutler et al. 2004); and Barbados, Tahiti, and Mururoa (Bard et al. 1998). A new reservoir age correction (Reimer et al. 2009) has been used for the corals from Barbados and Kirimati (Fairbanks et al. 2005), and Vanuatu and Papua New Guinea (Cutler et al. 2004). The planktonic foraminiferal records from the Cariaco Basin (varved sections from Hughen et al. [2000, 2004a,b] and non-varved sections tuned to the Hulu timescale from Hughen et al. [2006]), and from the Iberian Margin (non-varved sediments, tuned to the Hulu timescale: Bard et al. 2004a,b) are illustrated in Figure 7B. The results are also compared with the IntCal04 and IntCal09 calibration curves in Figure 7C. In addition, Figure 8 compares the results published more recently on the Bahamas and Hulu cave speleothems.

The Tahiti results will be discussed successively for 4 different time windows: (i) from 10 to 14.25 cal kyr BP, where our new data are in good agreement with previous data sets validated by the IntCal group; (ii) from 14.25 to 15.0 cal kyr BP, where the Tahiti record provides an improved description of the age plateau corresponding broadly to the Bølling-Allerød transition and MWP1-A period;
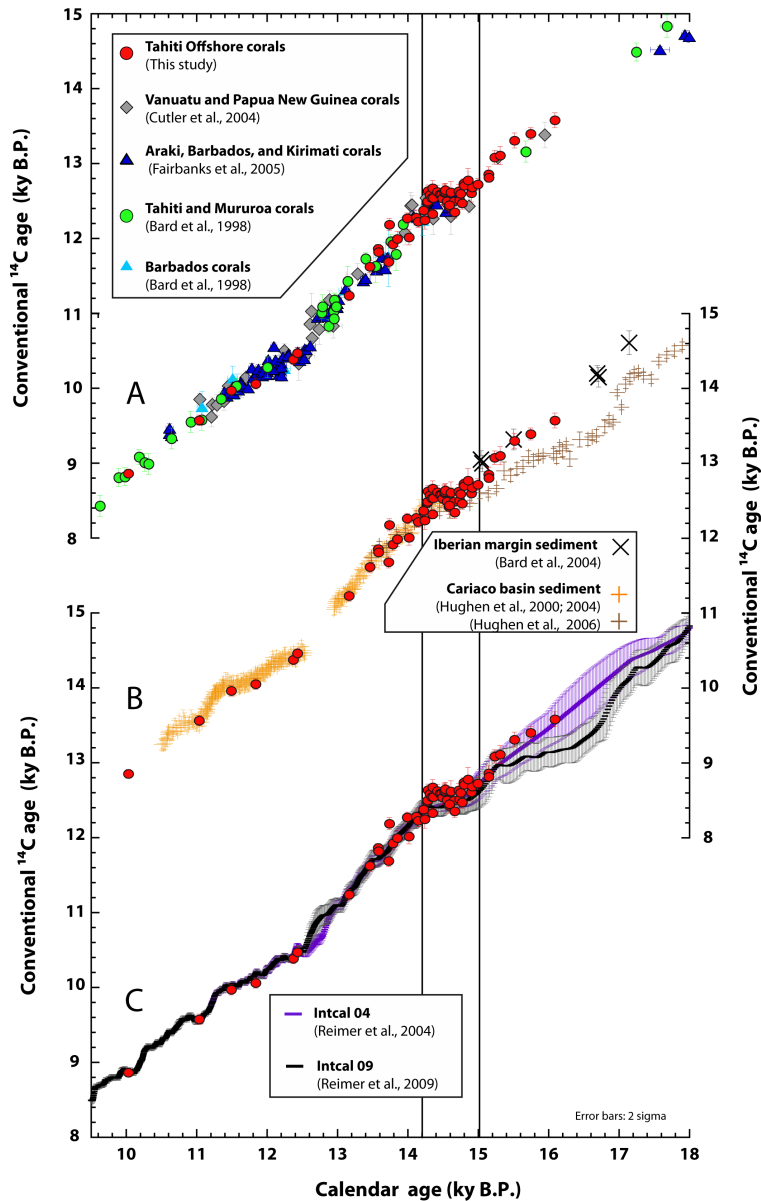
Figure 7 ^{14}C ages plotted versus calendar ages. ^{14}C ages are conventional ages in kyr BP corrected from the reservoir age. Tahiti data (red circles) have been corrected from a reservoir age of 300 yr (Bard et al. 1998). (A) Comparison of the new results from Tahiti with the other corals data sets: Araki, Barbados, and Kirimati (dark blue triangles, Fairbanks et al. 2005); Vanuatu and Papua New Guinea (gray diamonds, Cutler et al. 2004); Barbados (light blue triangles); Tahiti and Mururoa (green circles, Bard et al. 1998). These data have been corrected from the reservoir age adopted by the IntCal09 (Reimer et al. 2009). (B) Comparison of the new results from Tahiti with the marine sediment records. The foraminifera record from Cariaco Basin varved sediments (orange crosses, Hughen et al. 2000, 2004a,b), the foraminifera record from Cariaco Basin non-varved sediments (brown crosses, Cariaco Basin-Hulu timescale, Hughen et al. 2006), and the foraminifera record from Iberian Margin non-varved sediments (black crosses, Iberian Margin-Hulu timescale, Bard et al. 2004a,b). The error bars for ^{14}C ages and U-Th ages are also given at the 2σ level. (C) IntCal04 (purple) and IntCal09 (black) calibration curves (Reimer et al. 2004,2009).
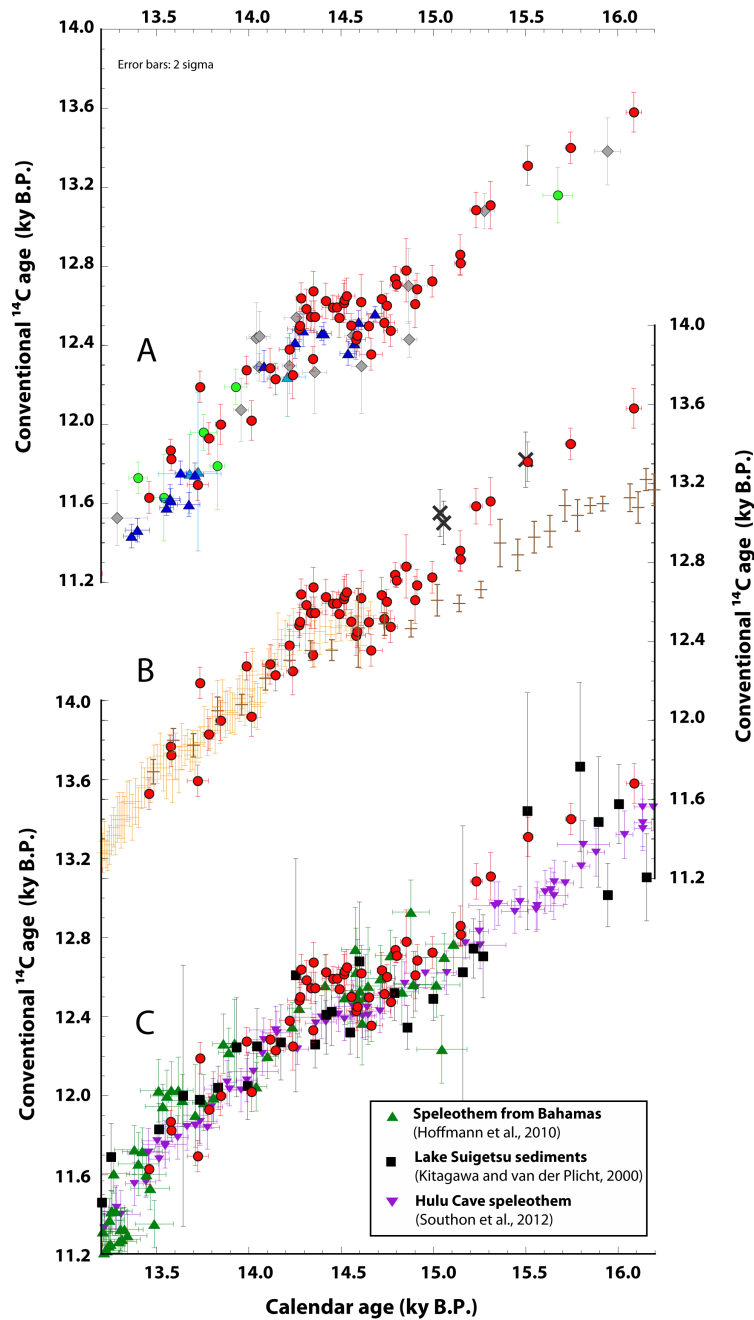
Figure 8 Blow-up of Figure 6 showing the 13.2–16.2 cal kyr BP interval. ¹⁴C ages plotted versus calendar ages. ¹⁴C ages are conventional ages in kyr BP and corrected for the reservoir age for the marine samples (see details in Figure 6 caption). Tahiti data are depicted by red circles. (A) Blow-up of Figure 6A between 13.2 and 16.2 cal kyr BP; (B) Blow-up of Figure 6B between 13.2 and 16.2 cal kyr BP; (C) Comparison of the new results from Tahiti with the speleothem data set from Bahamas (green triangles, Hoffmann et al. 2010), with the Hulu Cave speleothem record (purple inverted triangles, Southon et al. 2012), and with the Lake Suigetsu sediment record (black squares, Kitagawa and van der Plicht 2000). The error bars for ¹⁴C ages and U-Th ages are given at the 2σ level. As the error bars for ¹⁴C ages DCF-corrected for the Bahamas speleothem are large, the ¹⁴C age error is plotted without the propagation of the DCF incertitude for clarity.

(iii) from 15.0 to 16 cal kyr BP, where our results shed new light on the large discrepancy between the coral records and the Cariaco Basin sediment record; and (iv) from 29 to 37 cal kyr BP, where the Tahiti record provides only a few new data sets but are especially important in terms of calibration for this time window.

i) The time interval from 10 to 14.25 cal kyr BP was already well documented by 115 samples from previous coral records (see Reimer et al. 2009 and references therein). We add 20 new data for this period in very good agreement with all these previous records (Figure 7A). The new Tahiti results are also in good agreement with the Cariaco Basin sediment record within analytical uncertainty, except for 2 samples which are respectively slightly older (23 A 12.1 140-144) and younger (20 A 16.1 55-66) than the general trend depicted by the Cariaco record by about 1 century (Figure 7B). The good agreement between the Tahiti record and the previous coral records validates the reservoir correction used for this time period.

ii) The period from 14.25 to 15.0 cal kyr BP is characterized by a pronounced age plateau in the IntCal04 and IntCal09 calibration curves. As discussed in detail later, the 31 new Tahiti data sets we add to this interval enable us to refine the timing of this age plateau. We consider the broader interval, defined previously, in order to precisely compare the Tahiti results with: the 14 previous coral data available for this period (Figure 8A); with the Cariaco record (Figure 8B); with the Bahamas and Hulu cave speleothems (Hoffmann et al. 2010; Southon et al. 2012); and Lake Suigetsu sediments (Kitagawa and van der Plicht 2000) (Figure 8C). The shape of the plateau is now precisely constrained due to the enhanced resolution of our data over this time interval. When including all the 31 samples from 14.25 to 15.0 cal kyr BP, the average ^{14}C age is 12.577 ± 0.11 (1σ, $n = 31$). A linear fit through these points indicates a slope of 0.2, clearly lower than for the timespan before and after the plateau (slope of 0.87 and 0.76, respectively). The average ^{14}C age of the plateau, from 14.25 to 15.0 cal kyr BP, is somewhat older by about 120 yr than indicated by the Barbados and Vanuatu corals (12.457 ± 63, 1σ, $n = 8$ and 12.447 ± 161, 1σ, $n = 6$, respectively) (Figure 8A), the Cariaco record (Figure 8B), and lake Suigetsu sediments and Hulu Cave speleothem (Figure 8C). By contrast, the agreement is excellent with the Bahamas speleothem data (Figure 8C; 12.572 ± 0.132, $n = 16$). Nevertheless, in spite of these second-order differences, the main feature is that the average values of all these different records agree with each other within the 1σ uncertainty for the period from 14.25 to 15.0 cal kyr BP. As recorded by the Tahiti samples, the end of the plateau is clearly registered at 14.25 cal kyr BP (Figures 8 and 9). By contrast, the beginning of the plateau is much less defined due to the scarcity of coral samples: it starts between 14.6 and 14.7 cal kyr BP. Indeed, 5 samples dated between 14.5 and 14.7 cal kyr BP define a clear dip in the middle of the plateau, with ^{14}C ages 150 yr younger than others. As discussed later, these samples that could mark the beginning of the plateau, corresponding exactly to the occurrence of MWP-1A in the Tahiti sea-level record.

iii) In the period before the plateau, we dated 7 new samples from 16 to 15 cal kyr BP (Figure 8A). These results are in good agreement with the 3 coral data previously available during that period (2 from Vanuatu [Cutler et al. 2004] and 1 from Mururoa [Bard et al. 1998]).

The results are also in good agreement with the Iberian Margin record (Bard et al. 2004a,b within error at 15.5 cal kyr BP. At 15.0 kyr, Tahiti corals are younger than Iberian Margin ages by 300 ^{14}C yr (Figure 8B). By contrast, the coral data clearly mismatch with the Cariaco Basin record for that interval: while being essentially similar at the end of the plateau ~15 cal kyr BP, the Cariaco ages are already 400 yr younger than the corals at 16 cal kyr BP (Figure 8B). The difference increases towards older ages, and reaches 700 yr between the Cariaco and Iberian Margin record at 16.6 cal kyr BP (Figure 7B). The Hulu Cave data set (Southon et al. 2012) fits in an intermediate position between the Cariaco and coral data set (~200 yr younger than the latter all along that period; Figure 8C).

(iv) For the 29 to 37 cal kyr BP time period, the data provided by the Tahiti record are in good agreement with the corals from Barbados, except for the sample around 31 kyr BP (Figure 10). This last sample passed all our screening criteria but is in clear disagreement with the closest Tahiti data and with the Barbados data, so it can probably be considered an outlier. There are only a few new Tahiti data sets, but as the other coral data sets contain numerous gaps, each new measurement is crucial, as it contributes to improving the precision and the accuracy of the calibration curve for this time window. In addition, the good agreement between the 2 coral records validates the reservoir correction we used for this time period.

INTERPRETATION OF THE RESULTS

The compilation of ^{14}C-^{230}Th/U coral data over the entire deglaciation period shows only 2 prominent ^{14}C age plateaus (Figure 9A). These 2 intervals are thus characterized by abrupt decreases of the atmospheric Δ^{14}C (Figure 9B), with rates of decrease comparable to the radioactive decay (0.025‰/yr). These abrupt drops are superimposed on the long-term decrease of atmospheric Δ^{14}C over the past 40 kyr that is due in large part to the geomagnetic modulation of cosmogenic isotope production (Bard et al. 1990a; Frank et al. 1997; Bard 1998; Laj et al. 2002; Köhler et al. 2006).

The timing of the most recent plateau falls within the limits of the Younger Dryas (YD) climatic event. It began around 12.6 kyr BP after an initial Δ^{14}C rise of ~50‰ that occurred soon after the beginning of the Younger Dryas (YD) (Goslar et al. 1995; Hua et al. 2009). The end of the plateau occurred at ~11.5 cal kyr BP, broadly synchronous with the end of the YD event. The total decrease of atmospheric Δ^{14}C is ~100‰ during the YD ^{14}C age plateau (Figures 7A,B and 9B).

The oldest plateau is well documented by the new Tahiti record and corresponds to the transition between the Heinrich 1 and Bølling climatic events (Figure 9A and B). The end of the plateau is clearly registered between 14.25 cal kyr BP in the Tahiti data (Figure 8 and 9). By contrast, the beginning of the jump is much less defined due to the scarcity of coral samples. Its onset likely occurred between 14.7 and 14.6 kyr BP. This plateau corresponds to a sharp ^{14}C drop of ~100‰, synchronous with the onset of MWP-1A (Figure 11) (Deschamps et al. 2012). It is noteworthy that the ^{14}C drop and MWP-1A are evidenced with the same coral record providing unambiguous evidence for their synchronicity and likely highlighting a causal relationship between them. They are also coeval with the strengthening of the Atlantic Meridional Overturning Circulation (AMOC) based on the ^{231}Pa/^{230}Th ratio of North Atlantic sediments (McManus et al. 2004) (while the timing relationship between the ^{14}C record and the AMOC changes is different for the later YD event) and with the initial warming of the Bølling climatic phase as observed in Greenland ice cores (Rasmussen et al. 2006).

The available Tahiti data between 14.6–14.7 and 16.2 kyr BP are compatible with the other coral records and Iberian Margin sediment data (Figures 9, 11) By contrast, those ^{14}C data are all in significant contrast with the Cariaco record (Hughen et al. 2006), which exhibits a sharp 150‰ decrease between 16.5 and 15 kyr BP (Figures 9, 11). The new Hulu Cave speleothem record also shows a significant discrepancy (up to 60‰ ≈ 500 yr) with the Cariaco record, but it is also somewhat higher than several individual data from Tahiti corals and Iberian sediments (Figures 9, 11).

The residual discrepancy of ~300 yr between the Hulu and Tahiti data would disappear by assuming a larger reservoir age correction for Tahiti and/or a lower dead carbon fraction for the Hulu speleothems during the 17.5 to 15 kyr BP time window. At a low-latitude site like Tahiti, the only ways to increase the surface reservoir age are through upwelling of old water at the surface or by changing wind speed that controls the CO_2 exchange with the atmosphere (Bard 1988).
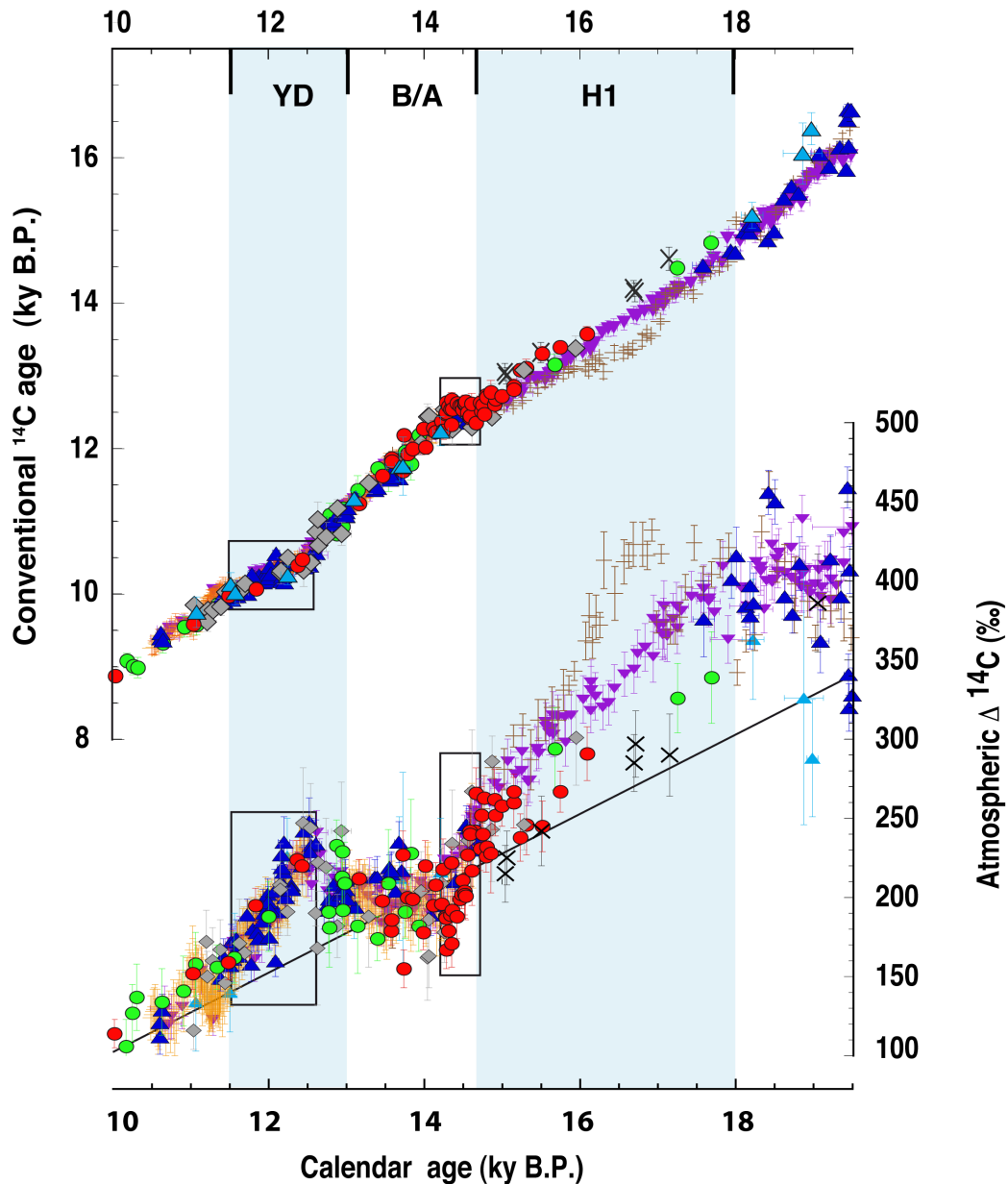
Figure 9 A) Occurrence of ^{14}C age plateaus for the whole deglaciation period. The different marine data sets are plotted together. The record based on Hulu Cave speleothem H82 (inverted purple triangles, Southon et al. 2012) has also been reported. The ^{14}C age plateaus in the calibration are marked with boxes, between 11.5 and 12.8 kyr BP and between 14.2 and 14.6 kyr BP. Symbols: same as in Figure 6; B) Atmospheric ^{14}C as calculated using the new ^{14}C results obtained on the corals from Tahiti plotted with the atmospheric ^{14}C calculated from the other records (Reimer et al. 2009) and with the ^{14}C record based on Hulu Cave speleothem H82 (Southon et al. 2012). The black boxes highlight the rapid drops in the atmospheric ^{14}C record corresponding to the ^{14}C age plateaus in A. The solid black line approximates the long-term trend of atmospheric [14]C. Symbols: same as in Figures 7 and 8. Labels under upper axis indicate significant climatic changes: H1, Heinrich event 1; B/A, Bølling-Allerød; YD, Younger Dryas.
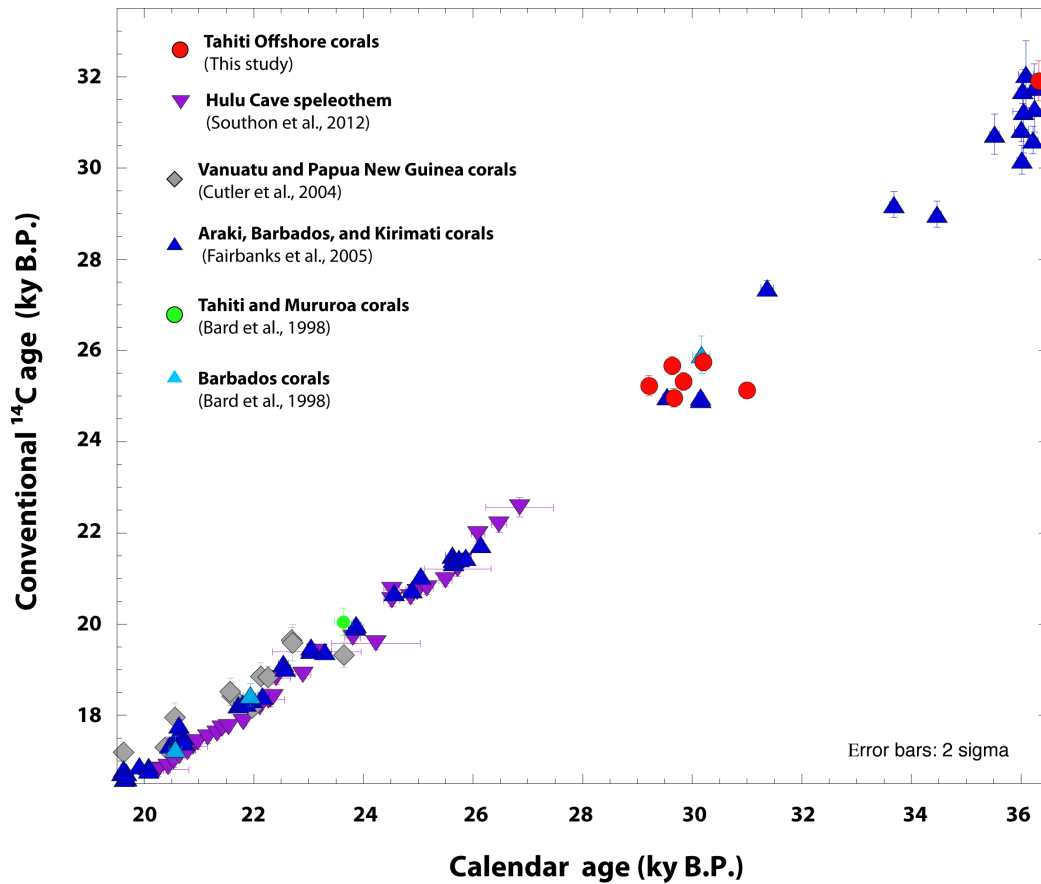
Figure 10 ^{14}C ages plotted versus calendar ages for the 20–36 kyr period. ^{14}C ages are conventional ages in kyr BP corrected from the reservoir age. Tahiti data (red circles) have been corrected from a reservoir age of 300 yr (Bard et al. 1998). Comparison of the new results from Tahiti with the other corals data sets: Araki, Barbados, and Kirimati (dark blue triangles, Fairbanks et al. 2005); Vanuatu and Papua New Guinea (gray diamonds, Cutler et al. 2004); Barbados (light blue triangles), Tahiti, and Mururoa (green circles, Bard et al. 1998). The error bars for ^{14}C ages and U-Th ages are given at the 2σ level.

The first effect can be illustrated by the corals from the Galapagos, which exhibit an average reservoir age of 500 yr (Druffel et al. 2004), thus larger than applied for Tahiti (300 yr). However, the location of the Galapagos Islands is very peculiar in the ocean, as it is influenced by old and nutrient-rich waters transported by currents from the eastern Pacific. By contrast, Tahiti is located within the main subtropical gyre of the South Pacific, a situation quite different from the Galapagos.

It is generally considered that wind speeds were higher during the last glacial period as a response to a steepened temperature gradient between low and high latitudes (Rea 1994; McGee et al. 2010). Increasing the wind-speed velocity by 50% on average would increase the CO_2 piston velocity, thereby leading to a reduction of the reservoir age by ~250 yr (Bard 1988). This first-order calculation based on a box-diffusion model is certainly a maximum value as increased wind speed also favors mixing with older water from below the surface box. In addition, the atmospheric CO_2 concentration was lower during the glacial period (190 vs. 280 ppm, Lourantou et al. 2010), which led to an increase of the reservoir age by ~175 yr for the full change between LGM and Holocene values (Bard 1988, 1998).
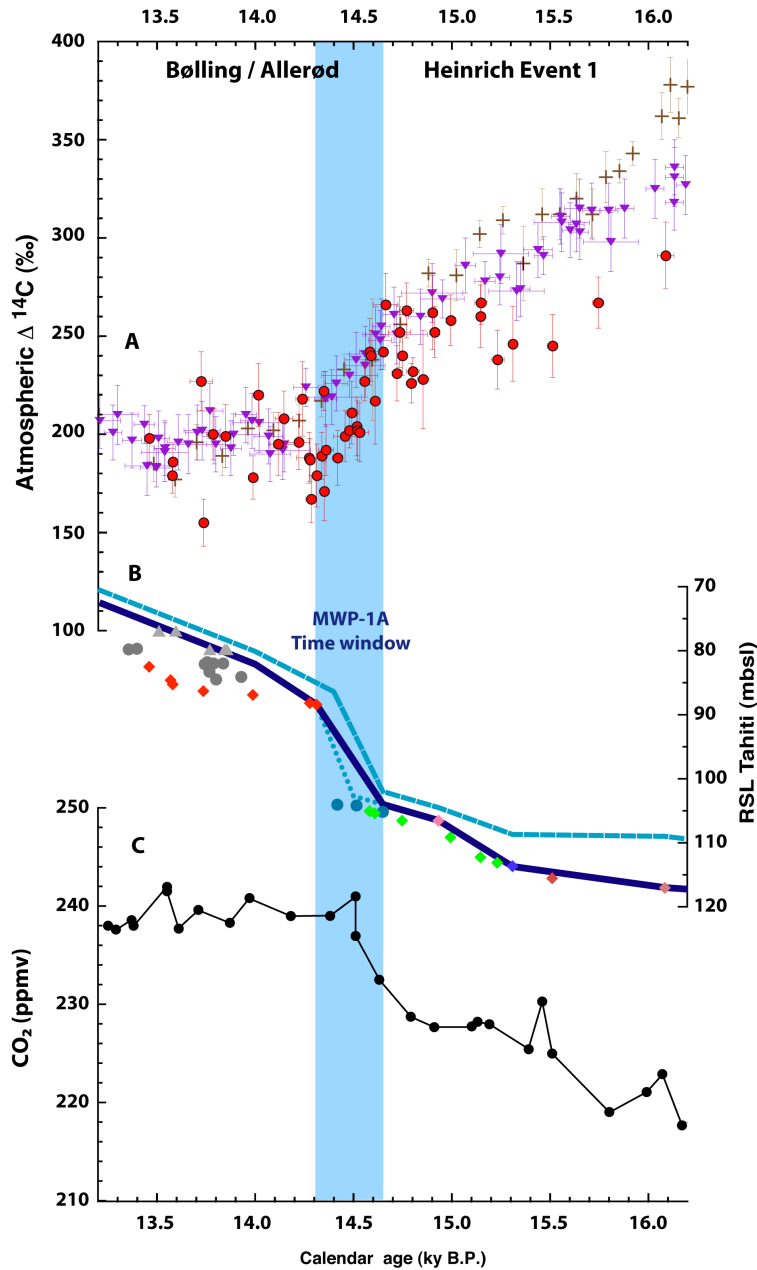
Figure 11 A) Atmospheric ^{14}C as calculated using the new ^{14}C results obtained on the corals from Tahiti (red circles) plotted with the atmospheric ^{14}C calculated from the Cariaco Basin record tuned to Hulu Cave (brown crosses, Hughen et al. 2006) and with the ^{14}C record based on Hulu Cave speleothem H82 (purple inverted triangles, Southon et al. 2012); B) Tahiti sea-level curve reconstructed from U-Th dated corals in long holes drilled onshore and offshore Tahiti Island (from Deschamps et al. 2012). Gray symbols correspond to coral samples collected in onshore holes (Bard et al. 1996, 2010), while colored symbols represent samples collected in offshore holes drilled during the IODP Expedition 310 (Deschamps et al. 2012). The thick blue line represents the lower estimate of the RSL curve. The occurrence of the MWP-1A is highlighted by the blue time window; C) Atmospheric CO_2 mixing ratio evolution during the last deglaciation. Data from EPICA Dome C and Talos Dome ice core (Lourantou et al. 2010; Schmitt et al. 2012).

In addition to these global changes in ^{14}C reservoir ages, we also need to take into account the possibility of local variations linked to regional climate changes, in particular during the H1 event. As shown by various isotopic proxies (Keigwin and Lehman 1994; McManus et al. 2004; Piotrowski et al. 2005), the AMOC was significantly reduced during this massive freshwater input to the North Atlantic. In the tropical Pacific, the main consequence was a southward shift of the Intertropical Convergence Zone (ITCZ) (e.g. Leduc et al. 2009), which probably affected the surface ocean circulation.

Maps of surface wind speed show that the ITCZ corresponds to a regional minimum between 2 maxima linked to the tradewind belts of the Northern and Southern hemispheres (e.g. Capps and Zender 2008). Consequently, a southward shift of the ITCZ might have led to a wind speed decrease in Tahiti. The direct effect would have been a decrease of the CO_2 piston velocity, leading to an increase of the reservoir age. For instance, a 25% decrease of local winds leads to an increase in reservoir age of 340 yr, enough to reconcile the Tahiti and Hulu data.

Other regional changes could have also influenced the tropical Pacific during glacial and deglacial periods. There is still a debate on the variability of ENSO during abrupt climatic changes identified in Greenland and the North Atlantic (e.g. Leduc et al. 2009). Nonetheless, a greater influence of ENSO in Tahiti (Felis et al. 2012) could have been accompanied by hydrological changes that may have affected the surface reservoir age.

Performing simulations with an ocean-atmosphere model is the only way to go beyond simple analogies with sites such as the Galapagos or first-order quantification of single processes with a box-diffusion model at steady state. Based on a model of intermediate complexity, Delaygue et al. (2003) showed that a strong meltwater discharge in the North Atlantic may lead to a transient decrease of up to 200 yr of the reservoir age of the equatorial Pacific. Butzin et al. (2005) performed simulations with a more sophisticated ocean model with various glacial conditions, including massive freshwater input into the North Atlantic. The tropical Pacific surface reservoir age exhibits a general increase by ~300 yr for glacial age conditions. However, freshwater injection experiments do not seem to produce large reservoir age changes, although Butzin et al. (2005) mention that regional-scale effects may not be fully captured by their model. As stressed by these authors, fully coupled ocean-atmosphere models are still needed to simulate in a realistic way the changes of the ocean surface ^{14}C ages. Such modeling work, beyond the scope of our paper, should help determine if the various effects mentioned above compensate each other or if a residual variation existed in Tahiti.

Variations of the reservoir age may have also affected the Cariaco record over the period corresponding to the H1 event, which could explain its discrepancy with other independent data (Tahiti corals, Iberian Margin sediments, and Hulu Cave speleothems). A similar problem was already observed for the first half of the YD event (Muscheler et al. 2008; Hua et al. 2009; Reimer et al. 2009). The proposed hypothesis is a transient reservoir age change at the site of Cariaco. The sign of the discrepancy implies that the ^{14}C reservoir age basically dropped to zero during half a millennium at this site. As explained above, an increase of wind velocity during the H1 interval might have caused a significant reduction of the reservoir age within the Cariaco Basin.

The H1 and YD share many similarities, so much so that some authors even use the term H0 for the YD. Both events are characterized by a reduced rate of ventilation of the deep ocean (Keigwin and Lehman 1994; McManus et al. 2004; Piotrowksi et al. 2005), which should have impacted the ^{14}C distribution between the surface and deep oceans. Consequently, a similar hypothesis could be proposed to explain the observed discrepancy during H1. However, the magnitude of the shift would imply that the reservoir age was negative at Cariaco, which seems unlikely. This problem is rein-

forced by the modeling work of Butzin et al. (2012) who showed that the reservoir age at Cariaco should have been larger during that time period, which would increase the discrepancy with other data.

In order to be exhaustive regarding the observed discrepancies during H1, it is important to mention the possibility of a bias in the Hulu Cave data. Similar to marine sediments, the ^{14}C ages are corrected for a dead carbon fraction (DCF). Southon et al. (2012) have shown that the DCF remained constant over a 3-kyr timespan between 10.7 and 13.9 kyr BP, including climatic periods such as the YD, the Allerød, and Early Holocene (characterized by dry or wet climate at this site; Wang et al. 2001). Although they admit that "the exceptional stability of the H82 DCF remains a puzzle," Southon et al. have assumed that it remained constant for older periods between 14 and 26 kyr BP. Besides the residual discrepancy with Tahiti data during the H1 event (see above), the Hulu data are also systematically younger (~300 yr) in ^{14}C than other available data between 20 and 26 kyr BP, corresponding to the last glacial maximum (corals from various sites and Lake Suigetsu varved sediments; cf. Figures 6 and 7 of Southon et al. 2012). One could invoke large changes of surface ocean reservoir ages at all sites, at the same time as missing varves in the lacustrine record (Kitagawa and van der Plicht 2000). A time-variable DCF would be a more parsimonious explanation, but it would imply a strongly reduced value during drier periods such as H1 and the LGM.

CONCLUSION

This work, based on the comparison of ^{14}C and U-Th ages in Tahiti coral samples, provides a new data set to the ^{14}C calibration for the last deglaciation period, including a higher resolution for the 14–16 cal kyr BP time interval. These new results are in good agreement with previous coral data sets and they extend the previous Tahiti records beyond 13.9 cal kyr BP, which was the oldest U-Th age obtained on cores drilled onshore in the modern Tahiti barrier reef.

The numerous data obtained for the 14–15 cal kyr BP time period enable us to refine the ^{14}C age plateau. This age plateau is associated with a period characterized by an abrupt decrease of atmospheric Δ^{14}C that might reflect changes in the global carbon cycle due to variations in the rates of exchange between the different carbon pools. It is difficult to directly evaluate the exact sequence of perturbations of the global carbon cycle, as well as their relationships with the abrupt events that punctuated the deglaciation, i.e. the Bølling warming, the MWP-1A event, and the increase of the atmospheric CO_2. The changes in strength or configuration of the deep-ocean circulation may have been the main causes of the observed variation of the Δ^{14}C during this time interval.

For the end of H1 period, the Tahiti record agrees with other corals and the Iberian Margin data sets but disagrees with the Cariaco Basin record. The observed discrepancies between the coral data set and the Cariaco Basin record could be related to changes in the western subtropical Atlantic reservoir ages during the mystery interval period, as was the case during the Younger Dryas event.

Numerical simulations by means of carbon cycle models should clarify the relationships between the fluctuations in ^{14}C records newly refined by the Tahiti record for the deglaciation period and changes in the global carbon cycle due to variations in the rates of exchange between the different carbon pools. In particular, the relation between the drop in ^{14}C record that produced the ^{14}C age plateau between 14–15 cal kyr BP and changes in the deep-ocean ventilation caused by the synchronous massive injection of melt water (MWP-1A) remain to be explored.

ACKNOWLEDGMENTS

REFERENCES

Andersen MB, Stirling CH, Potter E-K, Halliday AN. 2004. Toward epsilon levels of measurement precision on $^{234}U/^{238}U$ by using MC-ICPMS. *International Journal of Mass Spectrometry* 237:107–18.

Bard E. 1988. Correction of accelerator mass spectrometry ^{14}C ages measured in planktonic foraminifera: paleoceanographic implications. *Paleoceanography* 3(6):635–45.

Bard E. 1998. Geochemical and geophysical implications of the radiocarbon calibration. *Geochimica et Cosmochimica Acta* 62(12):2025–38.

Bard E, Hamelin B, Fairbanks RG, Zindler A. 1990a. Calibration of the ^{14}C timescale over the past 30,000 years using mass-spectrometric U-Th ages from Barbados corals. *Nature* 345(6274):405–10.

Bard E, Hamelin B, Fairbanks RG. 1990b. U-Th ages obtained by mass spectrometry in corals from Barbados: sea level during the past 130,000 years. *Nature* 346(6283):456–8.

Bard E, Hamelin B, Fairbanks RG, Zindler A, Mathieu G, Arnold M. 1990c. U/Th and ^{14}C ages of corals from Barbados and their use for calibrating the ^{14}C time scale beyond 9000 years B.P. *Nuclear Instruments and Methods in Physics Research B* 52(3–4):461–8.

Bard E, Arnold M, Fairbanks RG, Hamelin B. 1993. $^{230}Th/^{234}U$ and ^{14}C ages obtained by mass spectrometry on corals. *Radiocarbon* 35(1):191–9.

Bard E, Hamelin B, Arnold M, Montaggioni LF, Cabioch G, Faure G, Rougerie F. 1996. Deglacial sea-level record from Tahiti corals and the timing of global meltwater discharge. *Nature* 382(6588):241–4.

Bard E, Arnold M, Hamelin B, Tisnérat-Laborde N, Cabioch G. 1998. Radiocarbon calibration by means of mass spectrometric $^{230}Th/^{234}U$ and ^{14}C ages of corals: an updated database including samples from Barbados, Mururoa and Tahiti. *Radiocarbon* 40(3):1085–92.

Bard E, Ménot-Combes G, Rostek F. 2004a. Present status of radiocarbon calibration and comparison records based on Polynesian corals and Iberian Margin sediments. *Radiocarbon* 46(3):1189–202.

Bard E, Rostek F, Ménot-Combes G. 2004b. Radiocarbon calibration beyond 20,000 ^{14}C yr B.P. by means of planktonic foraminifera of the Iberian Margin. *Quaternary Research* 61(2):204–14.

Bard E, Hamelin B, Delanghe-Sabatier D. 2010. Deglacial Meltwater Pulse 1B and Younger Dryas sea levels revisited with boreholes at Tahiti. *Science* 327(5970):1235–7.

Butzin M, Prange M, Lohmann G. 2005. Radiocarbon simulations for the glacial ocean: the effects of wind stress, Southern Ocean sea ice and Heinrich events. *Earth and Planetary Science Letters* 235(1–2):45–61.

Butzin M, Prange M, Lohmann G. 2012. Readjustment of glacial radiocarbon chronology by self-consistent three-dimensional ocean circulation modeling. *Earth and Planetary Science Letters* 317–318:177–84.

Cabioch G, Banks-Cutler KA, Beck WJ, Burr GS, Corrège T, Edwards RL, Taylor FW. 2003. Continuous reef growth during the last 23 cal kyr BP in a tectonically active zone (Vanuatu, SouthWest Pacific). *Quaternary Science Reviews* 22(15–17):1771–86.

Camoin GF, Iryu Y, McInroy D, and the Expedition 310 scientists. 2007a. *Proceedings of the Integrated Ocean Drilling Program Management*. Volume 310: College Station: IODP International, Inc.

Camoin GF, Iryu Y, McInroy D, and the Expedition 310 scientists. 2007b. IODP Expedition 310 reconstructs sea-Level, climatic and environmental changes in the South Pacific during the Last Deglaciation. *Scientific Drilling* 5:4–12.

Capps SB, Zender CS. 2008. Observed and CAM3 GCM sea surface wind speed distributions: characterization, comparison, and bias reduction. *Journal of Climate* 21:6569–85.

Cardinal D, Hamelin B, Bard E, Patzold J. 2001. Sr/Ca, U/Ca and $\delta^{18}O$ records in recent massive corals from Bermuda: relationships with sea surface temperature. *Chemical Geology* 176(1–4):213–33.

Chen JH, Curran HA, White B, Wasserburg GJ. 1991. Precise chronology of the last interglacial period:

^{234}U-^{230}Th data from fossil coral reefs in the Bahamas. *Geological Society of America Bulletin* 103(1):82–97.

Cheng H, Edwards RL, Hoff J, Gallup CD, Richards DA, Asmerom Y. 2000. The half-lives of uranium-234 and thorium-230. *Chemical Geology* 169(1–2):17–33.

Condon DJ, McLean N, Noble SR, Bowring SA. 2010. Isotopic composition (^{238}U/^{235}U) of some commonly used uranium reference materials. *Geochimica et Cosmochimica Acta* 74(24):7127–43.

Cottereau E, Arnold M, Moreau C, Baqué D, Bavay D, Caffy I, Comby C, Dumoulin J-P, Hain S, Perron M, Salomon J, Setti V. 2007. Artemis, the new ^{14}C AMS at LMC14 in Saclay, France. *Radiocarbon* 49(2):291–9.

Cowan GA, Adler HH. 1976. The variability of the natural abundance of ^{235}U. *Geochimica et Cosmochimica Acta* 40(12):1487–90.

Cutler KB, Gray SC, Burr GS, Edwards RL, Taylor FW, Cabioch G, Beck JW, Cheng H, Moore J. 2004. Radiocarbon calibration to 50 kyr BP with paired ^{14}C and ^{230}Th dating of corals from Vanuatu and Papua New Guinea. *Radiocarbon* 46(3):1127–60.

Delanghe D, Bard E, Hamelin B. 2002. New TIMS constraints on the uranium-238 and uranium-234 in seawaters from the main ocean basins and the Mediterranean Sea. *Marine Chemistry* 80(1):79–93.

Delaygue G, Stocker TF, Joos F, Plattner GK. 2003. Simulation of atmospheric radiocarbon during abrupt oceanic circulation changes: trying to reconcile models and reconstructions. *Quaternary Science Reviews* 22(15–17):1647–58.

Deschamps P, Doucelance R, Ghaleb B, Michelot JL. 2003. Further investigations on optimized tail correction and high-precision measurement of Uranium isotopic ratios using Multi-Collector ICP-MS. *Chemical Geology* 201(1–2):141–60.

Deschamps P, Durand N, Bard E, Hamelin B, Camoin G, Thomas AL, Henderson GM, Okuno J, Yokoyama Y. 2012. Ice sheet collapse and sea-level rise at the Bølling warming, 14,600 yr ago. *Nature* 483(7391): 559–64.

Druffel ERM, Griffin S, Hwang J, Komada T, Beaupré SR, Druffel-Rodriguez KC, Santos GM, Southon J. 2004. Variability of monthly radiocarbon during the 1760s in corals from the Galapagos Islands. *Radiocarbon* 46(2):627–32.

Edwards RL, Chen JH, Ku T-L, Wasserburg GJ. 1987a. Precise timing of the Last Interglacial period from mass spectrometric determination of thorium-230 in corals. *Science* 236(4808):1547–53.

Edwards RL, Chen JH, Wasserburg GJ. 1987b. ^{238}U–^{234}U–^{230}Th–^{232}Th systematics and the precise measurement of time over the past 500,000 years. *Earth and Planetary Science Letters* 81(2–3):175–92.

Edwards RL, Beck JW, Burr GS, Donahue DJ, Chappell JMA, Bloom AL, Druffel ERM, Taylor FW. 1993. A large drop in atmospheric ^{14}C/^{12}C and reduced melting in the Younger Dryas, documented with ^{230}Th ages of corals. *Science* 260(5110):962–8.

Esat TM, Yokoyama Y. 2006. Variability in the uranium isotopic composition of the oceans over glacial–interglacial timescales. *Geochimica et Cosmochimica Acta* 70(16):4140–50.

Fairbanks RG, Mortlock RA, Chiu T-C, Cao L, Kaplan A, Guilderson TP, Fairbanks TW, Bloom AL, Grootes PM, Nadeau M-J. 2005. Radiocarbon calibration curve spanning 0 to 50,000 years BP based on paired ^{230}Th/^{234}U/^{238}U and ^{14}C dates on pristine corals. *Quaternary Science Reviews* 24(16–17):1781–96.

Felis T, Merkel U, Asami R, Deschamps P, Hathorne EC, Kölling M, Bard E, Cabioch G, Durand N, Prangue M, Schulz M, Cahyarini SY, Pfeiffer M. 2012. Pronounced interannual variability in tropical South Pacific temperatures during Heinrich stadial 1. *Nature Communications* 3:965, doi:10.1038/ncomms1973.

Frank M, Schwarz B, Baumann S, Kubik PW, Suter M, Mangini A. 1997. A 200 kyr record of cosmogenic radionuclide production rate and geomagnetic field intensity from ^{10}Be in globally stacked deep-sea sediments. *Earth and Planetary Science Letters* 149(1–4): 121–30.

Friedrich M, Lucke A, Hanisch S. 2004a. Late Glacial environmental and climatic changes from synchronized terrestrial archives of Central Europe: the Network PROSIMUL. *PAGES News* 12(2):27–9.

Friedrich M, Remmele S, Kromer B, Hofmann J, Spurk M, Kaiser KF, Orcel C, Küppers M. 2004b. The 12,460-year Hohenheim oak and pine tree-ring chronology from central Europe—a unique annual record for radiocarbon calibration and paleoenvironment reconstructions. *Radiocarbon* 46(3):1111–22.

Goslar T, Arnold M, Bard E, Kuc T, Pazdur MF, Ralska-Jasiewiczowa M, Tisnerat N, Rózański K, Walanus A, Wicik B, Wiêckowski K. 1995. High concentration of atmospheric ^{14}C during the Younger Dryas cold episode. *Nature* 377(6548):414–7.

Hoffmann DL, Beck JW, Richards DA, Smart PL, Singarayer JS, Ketchmark T, Hawkesworth CJ. 2010. Towards radiocarbon calibration beyond 28 ka using speleothems from the Bahamas. *Earth and Planetary Science Letters* 289(1–2):1–10.

Hogg AG, Turney CSM, Palmer JG, Fifield LK, Baillie MGL. 2006. The potential for extending IntCal04 using OIS-3 New Zealand sub-fossil kauri. *PAGES News* 14(3):11–2.

Hua Q, Barbetti M, Fink D, Kaiser KF, Friedrich M, Kromer B, Levchenko VA, Zoppi U, Smith AM, Bertuch F. 2009. Atmospheric ^{14}C variations derived from tree rings during the early Younger Dryas. *Quaternary Science Reviews* 28(25–26):2982–90.

Hughen KA, Overpeck JT, Lehman SJ, Kashgarian M, Southon JR, Peterson LC. 1998. A new ^{14}C calibration data set for the last deglaciation based on marine varves. *Radiocarbon* 40(1):483–94.

Hughen KA, Southon JR, Lehman SJ, Overpeck JT. 2000. Synchronous radiocarbon and climate shifts during the last deglaciation. *Science* 290(5498):1951–4.

Hughen KA, Southon JR, Bertrand CJH, Frantz B, Zermeño P. 2004a. Cariaco Basin calibration update: revisions to calendar and ^{14}C chronologies for core PL07-58PC. *Radiocarbon* 46(3):1161–87.

Hughen KA, Lehman S, Southon J, Overpeck J, Marchal O, Herring C, Turnbull J. 2004b. ^{14}C activity and global carbon cycle changes over the past 50,000 years. *Science* 303(5655):202–7.

Hughen KA, Baillie MGL, Bard E, Beck JW, Bertrand CJH, Blackwell PG, Buck CE, Burr GS, Cutler KB, Damon PE, Edwards RL, Fairbanks RG, Friedrich M, Guilderson TP, Kromer B, McCormac G, Manning S, Bronk Ramsey C, Reimer PJ, Reimer RW, Remmele S, Southon JR, Stuiver M, Talamo S, Taylor FW, van der Plicht J, Weyhenmeyer CE. 2004c. Marine04 marine radiocarbon age calibration, 0–26 cal kyr BP. *Radiocarbon* 46(3):1059–86.

Hughen K, Southon J, Lehman S, Bertrand C, Turnbull J. 2006. Marine-derived ^{14}C calibration and activity record for the past 50,000 years updated from the Cariaco Basin *Quaternary Science Reviews* 25(23–24): 3216–27.

Keigwin LD, Lehman SJ. 1994. Deep circulation change linked to HEINRICH event 1 and Younger Dryas in a middepth North Atlantic core. *Paleoceanography* 9(2):185–94.

Kitagawa H, van der Plicht J. 2000. Atmospheric radiocarbon calibration beyond 11,900 cal BP from Lake Suigetsu laminated sediments. *Radiocarbon* 42(3): 369–80.

Köhler P, Muscheler R, Fischer H. 2006. A model-based interpretation of low-frequency changes in the carbon cycle during the last 120,000 years and its implications for the reconstruction of atmospheric Δ^{14}C. *Geochemistry, Geophysics, Geosystems* 7: Q11N06, doi:10.1029/2005GC001228.

Laj C, Kissel C, Mazaud A, Michel E, Muscheler R, Beer J. 2002. Geomagnetic field intensity, North Atlantic Deep Water circulation and atmospheric Δ^{14}C during the last 50 kyr. *Earth and Planetary Science Letters* 200(1–2):177–90.

Leduc G, Vidal L, Tachikawa K, Bard E. 2009. ITCZ rather than ENSO signature for abrupt climate changes across the tropical Pacific? *Quaternary Research* 72(1):123–31.

Lourantou A, Lavric JV, Köhler P, Barnola J-M, Michel E, Paillard D, Raynaud D, Chappellaz D. 2010. A detailed carbon isotopic constraint on the causes of the deglacial CO$_2$ increase. *Global Biogeochemical Cycles* 24: GB2015, doi:10.1029/2009GB003545.

Mason AJ, Henderson GM. 2010. Correction of multi-collector-ICP-MS instrumental biases in high-precision uranium-thorium chronology. *International Journal of Mass Spectrometry* 295:26–35.

McGee D, Broecker WS, Winckler G. 2010. Gustiness: the driver of glacial dustiness? *Quaternary Science Reviews* 29(17–18):2340–50.

McManus JF, Francois R, Gherardi JM, Keigwin LD, Brown-Leger S. 2004. Collapse and rapid resumption of Atlantic meridional circulation linked to deglacial climate changes. *Nature* 428(6985):834–7.

Min GR, Edwards RL, Taylor FW, Recy J, Gallup CD, Beck JW. 1995. Annual cycles of U/Ca in coral skeletons and U/Ca thermometry. *Geochimica et Cosmochimica Acta* 59(10):2025–42.

Mook WG, van der Plicht J. 1999. Reporting ^{14}C activities and concentrations. *Radiocarbon* 41(3):227–39.

Muscheler R, Kromer B, Björck S, Svensson A, Friedrich M, Kaiser KF, Southon J. 2008. Tree rings and ice cores reveal ^{14}C calibration uncertainties during the Younger Dryas. *Nature Geoscience* 1:263–7.

Palmer J, Lorrey A, Turney CSM, Hogg A, Baillie M, Fifield K, Ogden J. 2006. Extension of New Zealand kauri (*Agathis australis*) tree-ring chronologies into Oxygen Isotope Stage (OIS) 3. *Journal of Quaternary Science* 21(7):779–87.

Paterne M, Ayliffe LK, Arnold M, Cabioch G, Tisnérat-Laborde N, Hatté C, Douville E, Bard E. 2004. Paired ^{14}C and ^{230}Th/^{230}U dating of surface corals from the Marquesas and Vanuatu (sub-equatorial Pacific) in the 3000 to 15,000 cal yr interval. *Radiocarbon* 46(2): 551–66.

Piotrowski AM, Goldstein SL, Hemming SR, Fairbanks RG. 2005. Temporal relationship of carbon cycling and ocean circulation at glacial boundaries. *Science* 307(5717):1933–8.

Rasmussen SO, Andersen KK, Svensson AM, Steffensen JP, Vinther B, Clausen HB, Siggaard-Andersen M-L, Johnsen SJ, Larsen LB, Dahl-Jensen D, Bigler M, Röthlisberger R, Fischer H, Goto-Azuma K, Hansson M, Ruth U. 2006. A new Greenland ice core chronology for the last glacial termination. *Journal of Geophysical Research* 111: D06102, doi: 10.1029/ 2005JD006079.

Rea DK. 1994. The paleoclimatic record provided by eolian dust deposition in the deep-sea the geologic history of wind. *Reviews of Geophysics* 32(2):159–95.

Reimer PJ, Hughen KA, Guilderson TP, McCormac G, Baillie MGL, Bard E, Barratt P, Beck JW, Buck CE, Damon PE, Friedrich M, Kromer B, Bronk Ramsey C, Reimer RW, Remmele S, Southon JR, Stuiver M, van der Plicht J. 2002. Preliminary report of the first workshop of the IntCal04 radiocarbon calibration/comparison working group. *Radiocarbon* 44(3):653–61.

Reimer PJ, Baillie MGL, Bard E, Bayliss A, Beck JW, Bertrand CJH, Blackwell PG, Buck CE, Burr GS, Cutler KB, Damon PE, Edwards RL, Fairbanks RG, Friedrich M, Guilderson TP, Hogg AG, Hughen KA, Kromer B, McCormac G, Manning S, Bronk Ramsey C, Reimer RW, Remmele S, Southon JR, Stuiver M, Talamo S, Taylor FW, van der Plicht J, Weyhenmeyer CE. 2004. IntCal04 terrestrial radiocarbon age calibration, 0–26 cal kyr BP. *Radiocarbon* 46(3):1029–58.

Reimer PJ, Baillie MGL, McCormac G, Reimer RW, Bard E, Beck JW, Blackwell PG, Buck CE, Burr GS, Edwards RL, Friedrich M, Guilderson TP, Manning S, Guilderson TP, Southon JR, Hogg AG, Stuiver M, Hughen KA, van der Plicht J, Kromer B, van der Plicht J, Manning S, Weyhenmeyer CE. 2006. Comment on "Radiocarbon calibration curve spanning 0 to 50,000 years BP based on paired ^{230}Th/^{234}U/^{238}U and ^{14}C dates on pristine corals" by R.G. Fairbanks et al. (Quaternary Science Reviews 24 (2005) 1781–1796) and "Extending the radiocarbon calibration beyond 26,000 years before present using fossil corals" by T.-C. Chin et al. (Quaternary Science Reviews 24 (2005) 1797–1808). *Quaternary Science Reviews* 25(7–8): 855–62.

Reimer PJ, Baillie MGL, Bard E, Bayliss A, Beck JW, Blackwell PG, Bronk Ramsey C, Buck CE, Burr GS, Edwards RL, Friedrich M, Grootes PM, Guilderson TP, Hajdas I, Heaton TJ, Hogg AG, Hughen KA, Kaiser KF, Kromer B, McCormac FG, Manning SW, Reimer RW, Richards DA, Southon JR, Talamo S, Turney CSM, van der Plicht J, Weyhenmeyer CE. 2009. IntCal09 and Marine09 radiocarbon age calibration curves, 0–50,000 years cal BP. *Radiocarbon* 51(4): 1111–50.

Robinson LF, Belshaw NS, Henderson GM. 2004. U and Th concentrations and isotope ratios in modern carbonates and waters from the Bahamas. *Geochimica et Cosmochimica Acta* 68(8):1777–89.

Schaub M, Buntgen U, Kaiser KF, Kromer B, Talamo S, Andersen KK, Rasmussen SO. 2008a. Lateglacial environmental variability from Swiss tree rings. *Quaternary Science Reviews* 27(1–2):29–41.

Schaub M, Kaiser KF, Frank DC, Buntgen U, Kromer B, Talamo S. 2008b. Environmental change during the Allerød and Younger Dryas reconstructed from Swiss tree-ring data. *Boreas* 37(1):74–86.

Schmitt J, Schneider R, Elsig J, Leuenberger D, Lourantou A, Chappellaz J, Köhler P, Joos F, Stocker TF, Leuenberger M, Fischer H. 2012. Carbon isotope constraints on the deglacial CO_2 rise from ice cores. *Science* 336(6082):711–4.

Seard C, Camoin G, Yokoyama Y, Matsuzaki H, Durand N, Bard E, Sepulcre S, Deschamps P. 2011. Microbialite development patterns in the last deglacial reefs from Tahiti (French Polynesia; IODP Expedition #310): implications on reef framework architecture. *Marine Geology* 279(1–4):63–86.

Sepulcre S, Durand N, Bard E. 2009. Mineralogical determination of reef and periplatform carbonates: calibration and implications for paleoceanography and radiochronology. *Global and Planetary Change* 66:1–9.

Shackleton NJ, Fairbanks RG, Chiu T-C, Parrenin F. 2004. Absolute calibration of the Greenland time scale: implications for Antarctic time scales and for ^{14}C. *Quaternary Science Reviews* 23(14–15):1513–22.

Southon J, Noronha AL, Cheng H, Edwards RL, Wang Y.

2012. A high-resolution record of atmospheric ^{14}C based Hulu Cave speleothem H82. *Quaternary Science Reviews* 33:32–41.

Stambaugh MC, Guyette RP. 2009. Progress in constructing a long oak chronology from the central United States. *Tree-Ring Research* 65(2):147–56.

Stirling CH, Esat TM, McCulloch MT, Lambeck K. 1995. High-precision U-series dating of corals from Western Australia and implications for the timing and duration of the Last Interglacial. *Earth and Planetary Science Letters* 135(1–4):115–30.

Stirling CH, Andersen MB, Potter EK, Halliday AN. 2007. Low-temperature isotopic fractionation of uranium. *Earth and Planetary Science Letters* 264(1–2): 208–25.

Stuiver M, Polach HA. 1977. Discussion: reporting of ^{14}C data. *Radiocarbon* 19(3):355–63.

Stuiver M, Reimer PJ, Bard E, Beck JW, Burr GS, Hughen KA, Kromer B, McCormac G, van der Plicht J, Spurk M. 1998. INTCAL98 radiocarbon age calibration, 24,000–0 cal BP. *Radiocarbon* 40(3):1041–83.

Thomas AL, Henderson GM, Deschamps P, Yokoyama Y, Mason AJ, Bard E, Hamelin B, Durand N, Camoin G. 2009. Penultimate deglacial sea-level timing from uranium/thorium dating of Tahitian corals. *Science* 324(5931):1186–9.

Vogel JS, Southon JR, Nelson DE, Brown TA. 1984. Performance of catalytically condensed carbon for use in accelerator mass spectrometry. *Nuclear Instruments and Methods in Physics Research B* 5(2):289–93.

Wang YJ, Cheng H, Edwards RL, An ZS, Wu JY, Shen C-C, Dorale JA. 2001. A high-resolution absolute-dated Late Pleistocene monsoon record from Hulu Cave, China. *Science* 294(5550):2345–8.

Weyer S, Anbar AD, Gerdes A, Gordon GW, Algeo TJ, Boyle EA. 2008. Natural fractionation of ^{238}U/^{235}U. *Geochimica et Cosmochimica Acta* 72(2):345–59.

Yokoyama Y, Esat TM. 2004. Long term variations of uranium isotopes and radiocarbon in the surface seawater recorded in corals. In: Shiyomi M, Kawahata H, Koizumi A, Tsuda A, Awaya Y, editors. *Global Environmental Change in the Ocean and on Land*. Tokyo: TERRAPUB. p 279–309.

Yokoyama Y, Esat TM, Lambeck K, Fifield LK. 2000. Last ice age millennial scale climate changes recorded in Huon Peninsula corals. *Radiocarbon* 42(3):383–401.

Yokoyama Y, Miyairi Y, Matsuzaki H, Tsunomori F. 2007. Relation between acid dissolution time in the vacuum test tube and time required for graphitization for AMS target preparation. *Nuclear Instruments and Methods in Physics Research B* 259(1):330–4.

Zhu ZR, Wyrwoll K-H, Collins LB, Chen JH, Wasserburg GJ, Eisenhauer A. 1993. High-precision U-series dating of Last Interglacial events by mass spectrometry: Houtman Abrolhos Islands, western Australia. *Earth and Planetary Science Letters* 118(1–4):281–93.

APPENDIX 1

Individual ^{14}C measurements. ^{14}C ages are conventional ages with a reservoir correction of 300 yr.

Sample	Lab code	^{14}C age (yr BP)	±2σ
310-M007A-18R-1W 76-90	SacA-11833	8875	60
310-M005A-12R-1W 51-54	SacA-10919	9585	70
310-M0018A-7R-1W 73-82	SacA-7268	9980	70
310-M005C-11R-1W 46-59	SacA-8563	10,070	70
310-M0023A-5R-1W 45-52	SacA-7282	10,395	70
310-M005D-2R-1W 107-115	SacA-7261	10,480	70
310-M005D-5R-2W 0-5	SacA-7258	11,245	70
310-M0023A-11R-1W 22-31	SacA-7257	11,630	80
310-M0015A-33R-1W 29-40	SacA-10915	11,970	100
310-M0015A-33R-1W 29-40	SacA-16816	11,820	70
310-M0023A-12R-1W 32-38	SacA-7263	11,850	80
310-M0023A-12R-1W 32-38	SacA-16817	11,800	80
310-M0020A-16R-1W 55-66	SacA-16841	11,695	80
310-M0023A-12R-1W 140-144	SacA-12016	12,190	80
310-M005D-6R-2W 0-5	SacA-7265	11,930	80
310-M009C-6R-1W 38-43	SacA-9087	12,000	100
310-M0023B-12R-1W 30-33	SacA-12017	12,275	70
310-M0021A-13R-2W 66-75	SacA-8579	12,020	100
310-M009E-7R-1W 5-13	SacA-9088	12,285	100
310-M0020A-21R-2W 13-20	SacA-7276	12,230	80
310-M009D-7R-1W 11-28	SacA-7269	12,380	80
310-M009A-6R-1W 38-48	SacA-18554	12,250	120
310-M0018A-18R-1W 40-50	SacA-8581	12,525	90
310-M0018A-18R-1W 40-50	SacA-10224	12,440	90
310-M0023B-12R-2W 113-127	SacA-8601	12,510	100
310-M0023B-12R-2W 113-127	SacA-10227	12,490	100
310-M0023B-15R-1W 0-5	SacA-8594	12,625	100
310-M0023B-15R-1W 0-5	SacA-10223	12,660	120
310-M0023A-13R-2W 32-37	SacA-10917	12,585	100
310-M0018A-19R-1W 107-110	SacA-7270	12,545	80
310-M009B-9R-2W 0-5	SacA-8592	12,280	100
310-M009B-9R-2W 0-5	SacA-16818	12,365	80
310-M0021B-16R-1W 39-44	SacA-10237	12,675	100
310-M009E-9R-1W 32-36	SacA-16849	12,545	80
310-M0015A-36R-1W 51-52	SacA-10239	12,625	90
310-M0020A-23R-1W 56-64	SacA-7278	12,625	80
310-M0020A-23R-1W 56-64	SacA-10225	12,540	100
310-M0025A-10R-1W 40-46	SacA-10235	12,690	100
310-M0025A-10R-1W 40-46	SacA-16819	12,545	70
310-M009D-9R-1W 66-77	SacA-8593	12,540	100

Individual ^{14}C measurements. ^{14}C ages are conventional ages with a reservoir correction of 300 yr. *(Continued)*

Sample	Lab code	^{14}C age (yr BP)	±2σ
310-M0015A-36R-2W 0-6	SacA-10240	12,615	100
310-M009B-13R-1W 11-18	SacA-10231	12,630	100
310-M009D-9R-1W 99-103	SacA-9111	12,650	90
310-M0016A-36R-2W 5-10	SacA-7279	12,510	80
310-M0016A-36R-2W 5-10	SacA-16820	12,490	90
310-M0024A-10R-1W 65-75	SacA-7281	12,430	100
310-M0023A-14R-1W 0-20	SacA-10918	12,450	80
310-M0024A-10R-1W 98-116	SacA-18555	12,620	140
310-M0015A-37R-1W 19-28	SacA-7275	12,465	80
310-M0015A-37R-1W 19-28	SacA-16821	12,530	80
310-M0020A-24R-2W 38-42	SacA-16840	12,355	80
310-M0026A-5R-1W 4-18	SacA-8562	12,635	90
310-M0020A-23R-2W 72-78	SacA-16848	12,515	100
310-M0024A-10R-2W 69-72	SacA-7260	12,635	80
310-M0024A-10R-2W 69-72	SacA-10226	12,550	100
310-M009E-9R-1W 69-73	SacA-16847	12,475	80
310-M009D-10R-2W 96-107	SacA-7277	12,730	80
310-M009D-10R-2W 96-107	SacA-10228	12,750	100
310-M0025B-9R-2W 60-70	SacA-8587	12,760	100
310-M0025B-9R-2W 60-70	SacA-13263	12,655	80
310-M0025B-9R-2W 60-70	SacA-13264	12,775	70
310-M0025B-9R-2W 60-70	SacA-13266	12,485	100
310-M0025B-9R-2W 60-70	SacA-1265	12,770	70
310-M0026A-5R-1W 117-127	SacA-18559	12,780	160
310-M0025B-10R-1W 0-5	SacA-9086	12,610	120
310-M009D-11R-1W 13-20	SacA-7267	12,685	80
310-M0024A-11R-2W 23-38	SacA-7256	12,725	80
310-M009B-14R-1W 22-25	SacA-10232	12,860	100
310-M0024A-13R-1W 32-41	SacA-7259	12,800	80
310-M0024A-13R-1W 32-41	SacA-10229	12,840	100
310-M0024A-14R-1W 24-28	SacA-10232	13,085	90
310-M0025B-11R-1W 70-74	SacA-8591	13,110	120
310-M009C-17R-2W 0-10	SacA-10233	13,310	100
310-M0024A-15R-1W 16-20	SacA-7264	13,400	80
310-M009B-15R-1W 13-20	SacA-8586	13,580	100
310-M009D-14R-2W 81-90	SacA-10234	25,230	220
310-M009B-16R-2W 13-17	SacA-13268	25,670	200
310-M009B-17R-1W 70-80	SacA-13267	24,960	200
310-M009B-17R-1W 5-10	SacA-9101	25,230	280
310-M009B-17R-1W 5-10	SacA-9102	25,420	280
310-M009D-18R-1W 19-28	SacA-13270	25,750	200
310-M009D-20R-2W 0-5	SacA-13269	25,130	100
310-M0025A-11R-1W 58-68	SacA-10236	31,910	440